POTENTIAL TLD MATERIALS FOR USE AS ULTRAVIOLET RADIATION DOSIMETERS

By

DICK ANDRIES SONO

Bachelor of Science
University of North West
Mafikeng, South Africa
1996

Bachelor of Science Honours
University of North West
Mafikeng, South Africa
1997

Submitted to the Faculty of the
Graduate College of the
Oklahoma State University
in partial fulfillment of
the requirements for
the Degree of
MASTER OF SCIENCE
May, 2000

POTENTIAL TLD MATERIALS FOR USE AS

ULTRAVIOLET RADIATION

DOSIMETERS

Thesis Approved:

Thesis Adviser

Dean of the Graduate College

ACKNOWLEDGEMENTS

I sincerely like to thank my advisor Dr Steve McKeever for the tremendous support he gave me through my studies. Sir, the patience you showed me kept me surviving and without you the whole research would have not been possible. Thank you.

To the physics faculty members, thanks very much for allowing me in the first place to be a member in your family. A special thanks goes to Dr Paul Westhaus for his never ending support and guidance. Sir you were always there when in need. Dr Martin, thanks for allowing me to use your lab. Thanks to Mike Lucas, for modeling some of the equipment I used during research.

To my colleagues in the lab, guys thanks very much for sharing and being so help with whatever the information you had. To the physics secretaries down stairs, ladies thanks for the help you gave me.

All the people who contributed to my stay at OSU, you made life easy for me here, Stillwater would have not been a bearable place without your support. Thank you.

Thanks to USAID and UNW for their continued financial support. Without you the whole thing could have been a dream.

Finally, I would like to thank my parents Mr Thomas M. and Lati V. Sono. The love you showed me since birth has no beginning or an end. You were always there when I needed you. My brothers and sisters thanks for the sacrifices and the courage you showed me through our childhood. Your moral support will always make a difference. A Modimo a nne le lona ba ga Sono. (May God be with you Sono's family).

THANKS BE TO GOD

TABLE OF CONTENTS

TABLE

LIST OF FIGURES

CHAPTER 1

1 ULTRAVIOLET DOSIMETRY USING THERMOLUMINESCENCE AND PHOTOTRANSFER THERMOLUMINESCENCE

1.1 Introduction

Ultraviolet (UV) radiation dosimetry using thermoluminescence has been of interest for some time due to increasingly common medical and industrial applications of ultraviolet radiation. Ultraviolet Radiation (UVR) is one of the non-ionizing radiations in the electromagnetic spectrum and can be classified into UVA (315-400nm), UVB (280-315nm) and UVC (100-280nm). Exposure to UVR occurs from both natural and artificial sources (i.e. various lamps used in medicine, commerce, research, industry and at home). In our environment the strongest source of UV is the sun and as sunlight passes through the atmosphere all UVC is absorbed and all except a small percentage of UVB is absorbed by the atmospheric component such as ozone, water vapor, oxygen and carbon dioxide [1& 2].

The effects of UVR have been studied by a number of researchers [1-5]. Driscoll [2] reported that an increased level of solar UVR due to stratospheric ozone layer depletion could have serious consequences for living organisms. A 10 % reduction in the ozone could lead to as much as 15-20% increase in effective UV exposure depending on the biological process being considered [1]. Adverse effects of increased exposure to UVB have been reported on plant growth, photosynthesis and disease resistance. Short term exposures to UVR induce feelings of well being and relaxation and further facilitate the synthesis of vitamin D [3& 4], however excess exposure affects the eyes increasing the

incidence of cataracts and skin cancer [1-5]. Both UVB and UVA appear to have a role to play in these effects. Studies in rodents and epithelial cells *in vitro* shows that exposure to UVA reduces survival of lens cells [5].

Radiation Dosimetry is the measurement of absorbed radiation dose in a material of interest. The detection and measurement of absorbed radiation was one of the earliest applications of thermoluminescence (TL). Thermoluminescence dosimeter (TLD) materials for monitoring ionizing radiation have been studied for their use as UV dosimeters by a number of researchers [16,29-36]. These dosimeters are often powders or pressed chips such as Al_2O_3, CaF_2, MgO, and LiF, doped with metal ion impurities.

The intrinsic UV response of some dosimeters is generally poor and preconditioning techniques such as pre-irradiation and preheating at high temperatures, has been investigated to enhance the UV sensitivity.

A survey was conducted with different TLD materials to find potential materials for use as UV Dosimeters. The materials used were: α-Al_2O_3:C, BeO, CaF_2 doped with Cu, Tm, Dy and Mn, $Li_2B_4O_7$:Mn, MgB_4O_7 doped with Mn, Tm and Dy, $CaSO_4$:Dy, MgO, MgO:Cu and LiF(DTG-4) from Russia equivalent to TLD-100 from Harshaw (USA). Most of the above materials were from Harshaw, USA. In the present study, phototransfer thermoluminescence (PTTL) was used as a dosimetry method in the UVB (307nm) region [16]. See description provided in the experimental part of the chapter 3. Only four materials viz. α-Al_2O_3:C from LC Technologies, USA, CaF_2:Cu of unknown origin, MgO and MgO:Cu both from Oak Ridge National Laboratory showed PTTL after UVB illumination for 1hr. Based on this observation, further experiments were performed only on these materials. NB. All the materials showed an appreciable TL

signal after 40Gy ^{60}Co irradiation at room temperature. Different thermal procedures were followed as recommended in McKeever et al [6].

Chapter 2 gives a detailed description of the models, mathematical approach and the processes involved in the production of thermoluminescence and phototransfer thermoluminescence (PTTL). It provides a clear definition of the terms TL and PTTL. The models are described starting with the simplest model (i.e. first-order model) for TL and extend to the general-order model. For PTTL, both the simplest model (i.e. the two traps/ one center-model) and more complex model (i.e. the two traps and two centres) as described by Alexander and McKeever [18] are furnished. The chapter also provides a treatment of the wavelength dependence of PTTL signal.

An overview of the TL and PTTL properties of the materials used in the study is provided in chapter 3. It also provides the description of the apparatus used and the experimental procedures followed.

The last chapter discusses the results of the materials studied with the exception of other materials* as obtained in the study. The results are presented starting from the TL of the materials, then PTTL as function of illumination time and re-use, then wavelength dependence. Included in this chapter is the summary of the whole study and a suggestion for future work.

*Material with no response to the 307nm UVB Dosimeter.

CHAPTER 2

2 THEORY OF THERMOLUMINESCENCE AND PHOTOTRANSFER THERMOLUMINESCENCE

2.1 THERMOLUMINESCENCE

2.1.1 Introduction

Thermoluminescence (TL) is the thermally stimulated emission of light following previous absorption of energy from radiation. When applied to radiation dosimetry the central objective of TL is to determine how much energy per unit mass (i.e. the dose) the material has absorbed during irradiation. According to McKeever et al. [6], this can be achieved by following the thermally stimulated release of the energy absorbed during heating of an irradiated sample by measuring the intensity of the emitted light. The emitted light, termed luminescence, is a result of relaxation of electronic charges from excited metastable state to the ground state, following initial absorption of energy from an external source. The absorption of energy causes the excitation of free electrons and free holes followed by the trapping of these electronic species at defects within the material.

Possibly the first scientific observation of TL was recorded by Robert Boyle 1663 (quoted in McKeever [7] and [8]), then Elsholtz 1676 (quoted in McKeever [8]), with the interpretation that heat was being converted to light. Du Fay 1738 provided a clear evidence that the phenomenon (TL) was more of a delayed phosphorescence and it was not until Wiedmann and Schimdt (1895) that the word "Thermoluminesncence" was

published in the literature (also quoted in McKeever [8]). Wiedmann and Schimdt induced TL by irradiation of sample with an electron beam in the laboratory as compared to the earlier observations of TL being induced by natural radioactivity from the environment.

2.1.2 First-Order Model

Randall and Wilkins [9,10] were the first to present a mathematical description of the TL phenomenon. They studied the thermal stability of trapped electrons and the probability of electron release from traps of different energy depths. The "depth" of a trap is the amount of thermal energy required to release the trapped charge into the delocalized bands. Their model was an electron-hole recombination model. Figure 2.1 illustrates the simplest possible model known as the one-trap/one center model. The probability of charge retrapping was assumed to be negligible as compared to the probability of recombination, and this lead to the " first-order " description of the TL process. The 'first-order' TL glow peak can be described by the following equations:

The probability per time (sec^{-1}) to release the trapped electron is

$$p(\mathrm{T}) = s \exp\left\{-\frac{E_t}{kT}\right\} \tag{1}$$

where k is Boltzmann's constant and T is the temperature. The pre-exponential factor s is a weakly dependent temperature term known as the "frequency factor " (often referred to as the "attempt-to-escape frequency"). Electrons absorb an amount of thermal energy sufficient to overcome the energy barrier E_t (the trap depth).

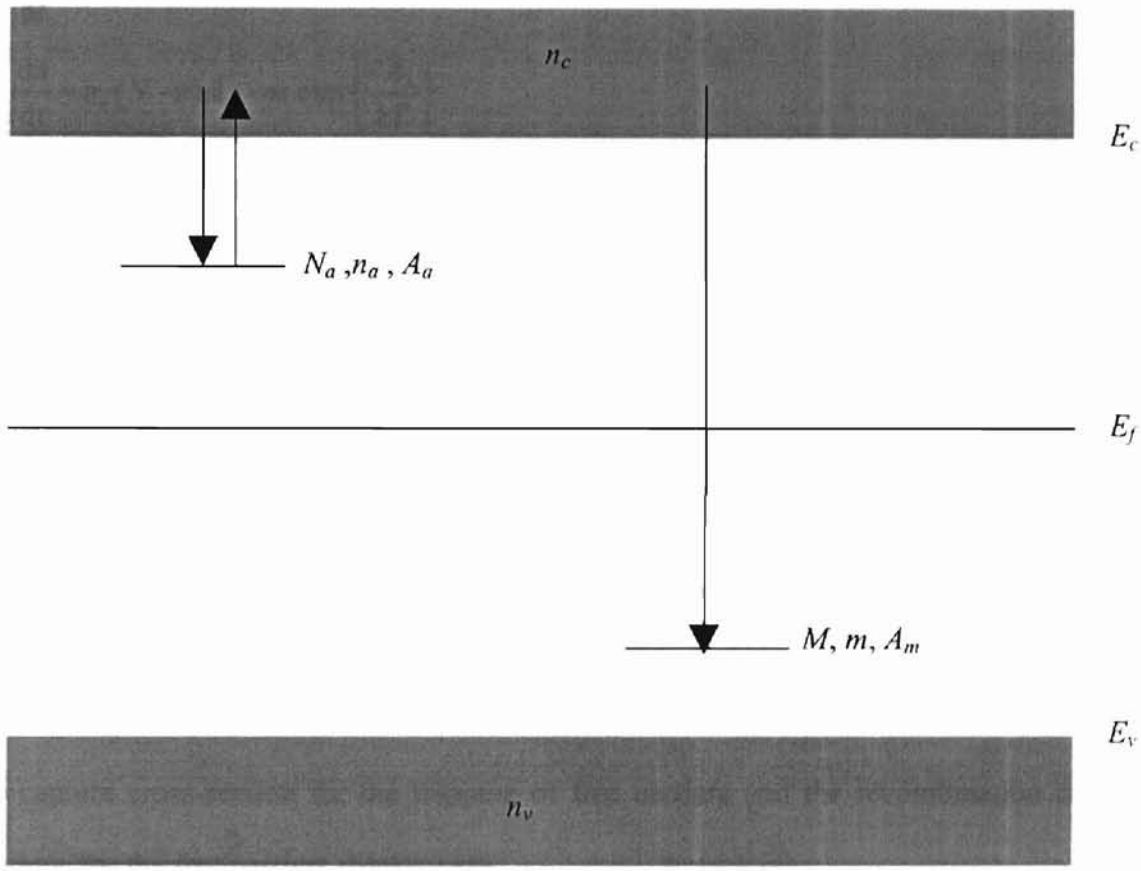

Figure 2.1. The allowed energy transition for the simple one-trap/one center model for TL. E_c and E_v are the conduction and valence band edges respectively. E_f is the Fermi level. The arrows indicate electron possible transitions.

The flow of electrons in or out of the delocalized bands during trap emptying (i.e. during heating) can be described by the following rate equations, from McKeever and Chen [12]

$$\frac{dn_c}{dt} = - n_c (N - n) A_n - ns \exp\left\{-\frac{E_t}{kT}\right\} - n_c m A_{mn} \tag{2}$$

$$\frac{dn_v}{dt} = 0 \tag{3}$$

$$\frac{dn}{dt} = n_c (N - n) A_n - ns \exp\left\{\frac{- E_t}{kT}\right\} \tag{4}$$

$$\frac{dm}{dt} = - n_c m A_{mn} \tag{5}$$

where the concentrations (per m^3) n_c, n and m are all time and temperature dependent. They are defined as follows: n_c is the number of free electrons in the conduction band, n_v is the number of holes in the valence band and n number of trapped electrons. N is the concentration of available electron traps and m is the concentration of recombination centres. $A_n = v_n \sigma_n$ and $A_{mn} = v_n \sigma_{mn}$ are the retrapping probability and recombination probabilities, respectively (all in $m^3\ s^{-1}$). v_n is the free electron velocity; σ_n and σ_{mn} are the capture cross-section for the trapping of free carriers and the recombination cross-sections for the free carriers respectively.

The above equations show that

$$\frac{dn_c}{dt} = \frac{dm}{dt} - \frac{dn}{dt} \tag{6}$$

The neutrality condition dictates that

$$n_c + n = m \tag{7}$$

Assuming the Randall and Wilkins first-order model, the rate of thermal excitation of electrons from the metastable trapping state to the excited state (i.e. the conduction band) is as follows;

$$\frac{dn}{dt} = - ns \exp\left\{-\frac{E_t}{kT}\right\} \tag{8}$$

where the negative sign signifies the loss of electrons. Assuming no retrapping, the electron will decay to the ground state (i.e. the valence band). In wide band insulator the decay to the ground state, however, proceeds by recombination of electrons with holes localized at the hole trapping states via a process known as the Hall-Schokley-Reed (HSR) process (from Chen and McKeever [11]). If the recombination is radiative, luminescence is emitted and the hole center is referred to as the luminescence center. The rate of decay (supply of electrons to the luminescence centre) is proportional to the intensity I (t) given by equation

$$I\,(\mathrm{t}) = - \eta \frac{dn}{dt} = - \eta\, ns \exp\left\{-\frac{E_t}{kT}\right\} \tag{9}$$

where η is a constant known as radiative efficiency. If all recombination events lead to photons produced by recombination events are detected then $\eta = 1$.

Integration of Eq. (8) yields

$$I\,(\mathrm{t}) = I_o \exp\{- tp\} \tag{10}$$

where I_o is the initial intensity at t = 0. An introduction of a quasiequilibrium (QE) approximation to these equations requires that the free electron concentration in the conduction band is quasistationary, that is:

$$\left|\frac{dn_c}{dt}\right| << \left|\frac{dn}{dt}\right|, \left|\frac{dm}{dt}\right| \tag{11}$$

This inequality leads to

$$\frac{dn}{dt} \approx \frac{dm}{dt} = I_{TL} \tag{12}$$

Applying the linear heating rate $\beta = dT/dt$, equation (9) can be solved as follows

$$\log\frac{n}{n_0} = -\int_{T_0}^{T} \beta^{-1} s \exp\left(-\frac{E_t}{kT}\right) dT \tag{13}$$

$$n = n_0 \exp\left\{-\int_{T_0}^{T} \beta^{-1} s \exp\left(-\frac{E_t}{kT}\right) dT\right\} \tag{14}$$

then from equation (9)

$$I_{TL}(\mathrm{T}) = n_0 s \exp\left\{-\frac{E_t}{kT}\right\} \exp\left\{-\int_{T_0}^{T} \beta^{-1} s \exp\left(-\frac{E_t}{k\theta}\right) d\theta\right\} \tag{15}$$

Without any loss of generality equation (16) can be written as

$$I_{TL}(\mathrm{T}) = n_0 s \exp\left\{-\frac{E_t}{kT}\right\} \exp\left\{-\int_{T_0}^{T} \beta^{-1} s \exp\left(-\frac{E_t}{k\theta}\right) d\theta\right\} \tag{16}$$

where n_0 is the initial filled electron traps at $t = 0$, $T = T_0 + \beta t$ and θ is a dummy variable representing temperature. Using this equation a characteristic " first-order" TL glow curve can be plotted. Figure 2.2 illustrates the first-order and second-order TL glow peaks. First-order expression (curve I) is characterized by asymmetry of the TL glow curve.

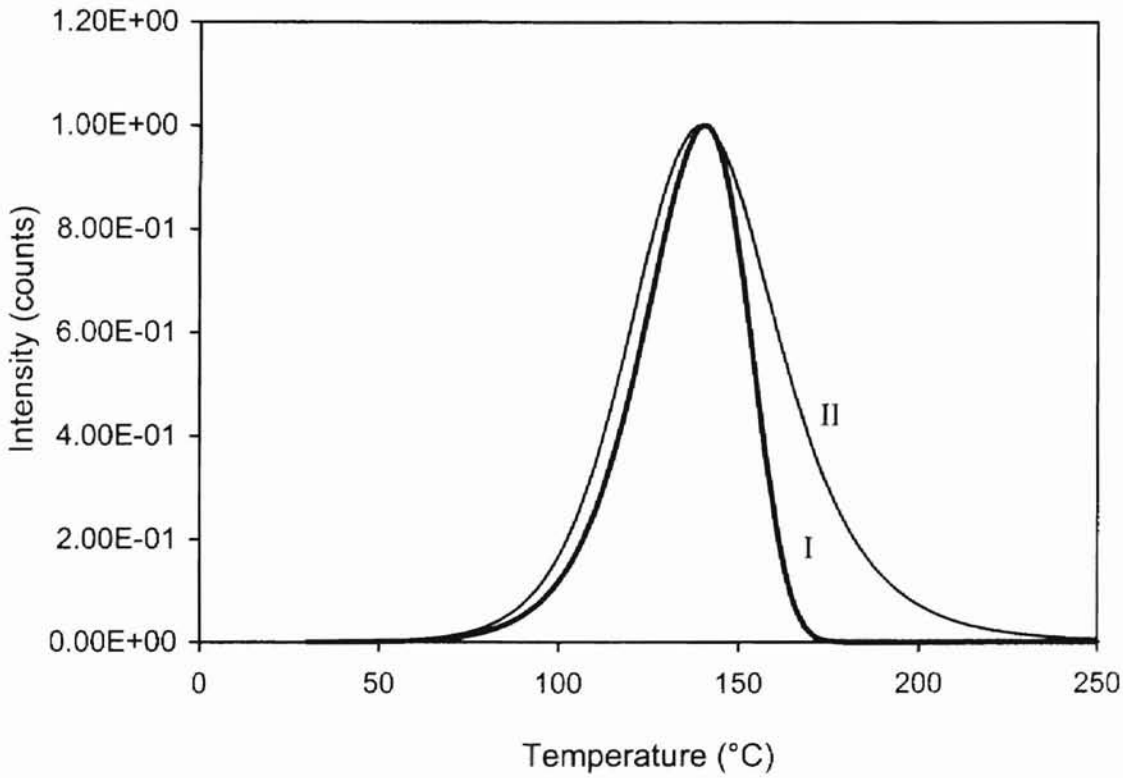

Figure 2.2. Normalized simulation of the first- and second-order TL glow curves calculated with E_t = 1.0 eV, s = 10^{11} s^{-1}, and β = 1.0°C s^{-1}. For the second-order curve (II) peak n_0/N = 1

2.1.3 Second-Order Model

Later Garlick and Gibson [13] modified the model (first-order) to a "second-order" TL process comparing the probabilities of retrapping and recombination. The model describes the probability of electrons being trapped in the metastable state or recombine in the ground state. Under such conditions

$$I(t) = -\eta \frac{dn}{dt} = \alpha n^2 \tag{17}$$

where α is a constant at constant temperature T. The constant α is related to the mean time electron spends in the metastable state and it describes the relative probabilities of retrapping at the metastable state and recombination at the ground state. Comparison of equation (9) and (17) shows that the rate of decay is proportional to the n^2 rather than n, hence "second-order".

Using the possibility that retrapping dominates recombination, i.e. $m\sigma_{mn} << (N - n)\sigma_n$, we have (from Chen and McKeever [11])

$$I_{TL}(T) = -\frac{dn}{dt} = s\left(\frac{\sigma_n}{N\sigma_{mn}}\right) n^2 \exp\left\{-\frac{E_t}{kT}\right\} \tag{18}$$

Integration yields

$$I_{TL}(T) = \left(\frac{n_0{}^2\sigma_n}{N\sigma_{mn}}\right) s \exp\left\{-\frac{E_t}{kT}\right\} \left[1 + s\left(\frac{n_0\sigma_n}{\beta N\sigma_{mn}}\right)\int_{T_0}^{T} \exp\left\{-\frac{E_t}{kT}\right\} d\theta\right]^{-2} \tag{19}$$

This equation is the Garlick-Gibson equation for second-order TL glow curve. Using the assumption that σ_n / σ_{mn} is unity, then Eq. (19) becomes

$$I_{TL}(\mathrm{T}) = \left(\frac{n_0^2}{N}\right) s \exp\left\{-\frac{E_t}{kT}\right\}\left[1 + s\left(\frac{n_0}{\beta N}\right)\int_{T_0}^{T}\exp\left\{-\frac{E_t}{kT}\right\}\mathrm{d}\theta\right]^{-2} \tag{20}$$

Figure 2.2 shows characteristics of "second-order" glow peak. When compared with the first order TL curve, "second-order" peak is wider and more symmetric. This is because of the fact that significant concentration of electrons are re-trapped before they recombine, giving rise to a delay in the luminescence emission and a spreading out of the emission over a wider temperature (Chen and McKeever [11]).

2.1.4 General-Order Kinetics

For the first-order and second-order models inequalities were assumed regarding the probabilities of retrapping and recombination. The inequalities assumed in the models are not always applicable in practice. May and Patridge [14] generalized equations (8) and (18) in order to apply them to cases were the inequalities assumed above were not applicable. The empirical expression written by them for the general-order TL kinetics, is thus

$$T_{TL} = n^{l} s' \exp\left\{\frac{-E_t}{kT}\right\} \tag{21}$$

where l is defined as the general-order parameter and $s' = n/N$ has dimensions of $\mathrm{m}^{3(l-1)}\mathrm{s}^{-1}$.

For $l \neq 1$, integration of (21) yields

$$T_{TL} = n_0 s'' \exp\left\{\frac{-E_t}{kT}\right\}\left[1 + (l-1)\frac{s''}{\beta}\int_{T_0}^{T}\exp\left\{-\frac{E_t}{k\theta}\right\}\mathrm{d}\theta\right]^{-\frac{l}{l-1}} \tag{22}$$

where $s'' = s' n_0^{(l-1)}$ and n_0 is the electron concentration at T_0. According to Rasheedy (1993) described in Chen and McKeever [11], Eq. 21 can be amended to overcome the difficulty with the empirical development of the strange units of the parameter s', thus

$$T_{TL} = -\frac{dn}{dt} = \frac{n^l}{N^{l-1}} s \exp\left\{\frac{-E_t}{kT}\right\} \tag{23}$$

For l=1 and l=2 Eq.23 reduces to first-order and second-order cases respectively. Integration yields

$$T_{TL} = n_0^l s \exp\left\{\frac{-E_t}{kT}\right\} N^{(1-l)} \left[1 + (l-1)\frac{s(n_0/N)^{(l-1)}}{\beta} \int_{T_0}^{T} \exp\left\{-\frac{E_t}{k\theta}\right\} d\theta\right]^{-\frac{l}{l-1}} \tag{24}$$

The intensity of the thermally stimulated luminescence is now proportional to the l^{th} - order kinetic function. Both Eq. 22 and 24 reduce to Randall Wilkins first-order equation as $l \to 1$.

2.2 PHOTOTRANSFER THEMOLUMINESCENCE

Phototransfer thermoluminescence (PTTL) is a TL signal observed from optically induced transfer of charge from deeper to shallow traps in insulating or semiconducting materials. The observation of PTTL has lead to the phenomenon being used as a useful technique in dating and radiation dosimetry (McKeever, [8]). For a given illumination power and exposure time, PTTL is proportional to the initial absorbed dose (i.e. the amount of radiation initially absorbed by the material) (McKeever et al [6]). It is necessary for the material to be pre-exposed to radiation and that the annealing conditions necessary for re-use do not empty the deep source traps from which the PTTL signal is

transferred. PTTL has been studied in many materials, including LiF, CaF_2, Al_2O_3, quartz and diamonds. PTTL from quartz has been studied due to its potential as a tool in archaeological and geological dating (Wintle and Murray, [22]).

One of the common procedures to observe PTTL is to irradiate the TL material at a temperature T_{irr}. After irradiation the material is pre-heated to a temperature T_{ph} sufficient to remove charge from the acceptor trap. The donor traps remain populated during this process. The material is then cooled back to T_{irr}, at this stage it is illuminated with light of a wavelength sufficient to excite the charge from the deep donor traps to the acceptor traps. Subsequent heating of the material after illumination shows a TL signal due to thermal release of charge from the acceptor traps. For a given radiation dose, the PTTL signal is proportional to the illumination time.

2.2.1 The Simplest Model

The simplest possible model to describe PTTL (Chen and McKeever [11], Alexander and McKeever [19]), is that of a two traps and one centre, viz. one shallow trap into which the charge is transferred (acceptor trap), one deep trap from which the charge is excited (source or donor trap), and one recombination center (hole trap; for luminescence). Figure 3 shows possible transfer of electrons in the model. The condition imposed for PTTL is the initial condition that $n_{a0} = 0$ and $n_{d0} = m_0$ after irradiation and immediately before illumination. The transfer of charge from the donor traps into the acceptor traps during illumination may be described by the following set of rate equations

$$\frac{dn_a}{dt} = A_a(N_a - n_a)n_c - f_a n_a \tag{25}$$

$$\frac{dn_d}{dt} = A_d(N_d - n_d)n_c - f_d n_d \tag{26}$$

$$\frac{dm}{dt} = -A_m m n_c = \frac{m}{\tau} \tag{27}$$

where τ is the recombination lifetime, $f_d = \phi(\lambda)\sigma_d(\lambda)$ is the rate at which electrons are lost from the deep, donor trap and $f_a = \phi(\lambda)\sigma_a(\lambda)$ is the rate loss of electrons from the shallow, acceptor traps. Both f_d and f_a are due to optical excitation. $\phi(\lambda)$ is the intensity of excitation light, σ_d and σ_a are the photo-ionization cross section from the deep donor traps and shallow acceptors traps respectively. The concentrations (m^{-3}) are defined as follows; let N_a be the concentration of available shallow acceptor traps, N_d is the concentration of deep donor traps and M concentration of the recombination center. The concentrations n_a, n_d and m are the concentrations (m^{-3}) of electrons or holes trapped at these centres respectively; n_c is the concentration of free electrons. A_a and A_d are the probabilities ($m^3\ s^{-1}$) for trapping of free charges in the empty traps and A_m is the probability of a free electron recombining with a trapped hole at the recombination centre. Charge neutrality dictates that

$$n_c + n_a + n_d = m. \tag{28}$$

In order to observe the PTTL signal the sample is heated and during heating, the electrons will thermally escape from shallow acceptor traps and may either recombine with the trapped holes to yield PTTL signal or be retrapped in the deep donor traps. This process can now be represented by the following rate equations

$$\frac{dn_c}{dt} = \frac{dm}{dt} - \frac{dn_a}{dt} - \frac{dn_d}{dt} \tag{29}$$

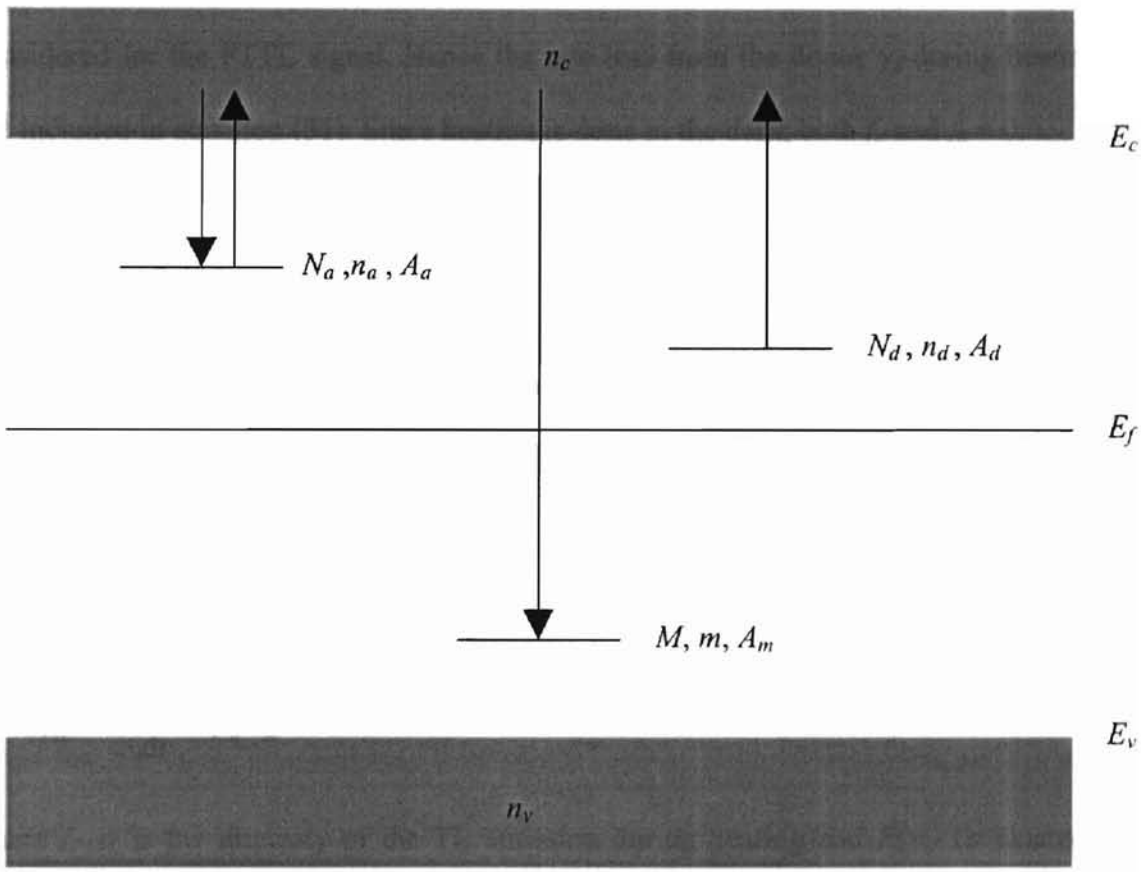

Figure 2.3. The simple PTTL model. E_c and E_v are the conduction and valence band edges respectively. E_f is the Fermi level. The arrows indicate the possible electron transitions.

$$\frac{dn_a}{dt} = A_a(N_a - n_a)n_c - \gamma_a\ n_a \tag{30}$$

$$\frac{dn_d}{dt} = A_d(N_d - n_d)n_c \tag{31}$$

$$\frac{dm}{dt} = -A_m m n_c = \frac{m}{\tau} \tag{32}$$

where the optical detrapping term f_a is replaced by the thermal detrapping term γ_a. The temperature range is such that the thermal emptying from the source or donor traps is not considered for the PTTL signal. Hence the rate loss from the donor γ_d during heating is not included in equation (31). Since heating is done in the dark, both f_d and $f_a = 0$.

The thermal excitation has the form

$$\gamma_a = s_a\ \exp\left\{-\frac{E_a}{kT}\right\} \tag{33}$$

where s_a and E_a are the frequency factor and energy depth of the acceptor trap respectively. Assuming quasiequilibrium and no retrapping into the source traps ($n_a\gamma_a >> A_a\ (N_a - n_a)\ n_c$), the solutions to the above equations are as follows

$$I_{PTTL} = -\frac{dm}{dt} = \gamma_a A_m m F(m) \tag{34}$$

where I_{PTTL} is the intensity of the TL emission during heating and $F(m)$ (evaluated by Alexander and McKeever, [19]) can be written as

$$F(m) = [(n_{a0} + n_{d0} - m_0 - N_d) + m + (N_d - n_{d0})(m/m_0)^{A_d/A_m}] \times$$
$$[A_a(N_a + N_d - n_{a0} - n_{d0} + m_0) + (A_m - A_a)(N_d - n_{d0})(m/m_0)^{A_d/A_m}]^{-1} \tag{35}$$

Equation (34) and (35) were solved only with the assumption of quasiequilibrium, but can be further simplified by introduction of additional assumptions. By using a linear heating rate $\beta = \mathrm{d}T / \mathrm{d}t$, equation (34) can be written with a change of variable from t to T as follows

$$I_{PTTL} = -\beta \frac{\mathrm{d}m}{\mathrm{d}T} = \beta \gamma_a A_m m F(m) \tag{36}$$

then

$$S_{PTTL} = \int_{T_0}^{T_f} I_{PTTL} \mathrm{d}T \tag{37}$$

where S_{PTTL} is defined as the area under the PTTL curve, integrated between the initial temperature T_0 and the final temperature T_f. Under the conditions of retrapping into the deep donor traps and the assumption that $n_{a0} << N_d - n_{d0}$, equations (29), (30), and (32), can be combined to give

$$S_{PTTL} \approx \frac{A_m m_0 n_{a0}}{A_d (N_d - n_{d0})} \tag{38}$$

Due to the competing effect of the donor traps during thermal trapping, it should be noted that the S_{PTTL} is not simply proportional to the electron concentration n_{a0} in the acceptor trap at the end of illumination period. Under the assumption that retrapping into donor traps was negligible ($\mathrm{d}n_d/\mathrm{d}t << \mathrm{d}m/\mathrm{d}t$, $\mathrm{d}n_a/\mathrm{d}t$), it can be assumed that

$$S_{PTTL} = \beta \int_{T_0}^{T_f} \frac{\mathrm{d}m}{\mathrm{d}t} T = m_0 - m_f \propto n_{a0} \tag{39}$$

To use equations (38) and (39) to determine the dependence of the PTTL signal as a function of the illumination time, the variation of $n_{a0}(t)$, $n_{d0}(t)$ and $m_0(t)$, with illumination time has to be known.

An alternative to determining the PTTL, as function of illumination time is that assumed by Wintle and Murray [22], in which the rate equations to describe the process are as follows;

$$\frac{dn_d}{dt} = -f_d n_d \tag{40}$$

$$\frac{dn_a}{dt} = af_d n_d - f_a n_a \tag{41}$$

where f_d and f_a are defined as before (i.e. the rate loss of electron from the deep, donor traps and rate loss from the shallow, acceptor traps respectively). The solution to equation (40) and (41) is

$$n_a = \frac{af_d n_{d0}}{f_a - f_d}[\exp(-f_d t) - \exp(-f_a t)] \tag{42}$$

Combining equation (39) and (42)

$$S_{PTTL} = C\frac{af_d n_{d0}}{f_a - f_d}[\exp(-f_d t) - \exp(-f_a t)] \tag{43}$$

where C is the proportionality constant. For $f_a = 0$, equation (43) becomes

$$S_{PTTL} = Cn_{d0}[1 - \exp(-f_d t)] \tag{44}$$

As described by Alexander and McKeever [19], the shape of equation (42) is characterized by an increase followed by decrease to an eventual zero level. The

interpretation being illumination in addition to filling the acceptor traps, is also emptying these traps via optical bleaching. However, it is uncertain whether illumination does in fact optically empty the acceptor traps in all materials. Therefore, the validity of equation (42) is dependent upon the particular system being examined experimentally.

2.2.2 The Complex Model

The description of the PTTL using this model (i.e. two traps and two centres) follows the principle described by Alexander and McKeever [19]. In the simple model the PTTL versus time curve followed an increase then a decrease to zero after long illuminations. This is possible if the decrease was due to optical excitation of charge from the shallow, acceptor trap during illumination. For cases were the curve first increases, then decreases, and follows a steady state level that is not zero at long illumination times, simple model described above does not hold. The authors introduced a second recombination centre that was assumed to be non-radiative and an additional deep trap. The deep trap is not optically active and it was introduced to explain sensitivity changes [35]. Recombination at the second centre produces only phonons.

The rate equations describing the possible processes are as follow;

$$\frac{\mathrm{d}n_c}{\mathrm{d}t} = R - \frac{\mathrm{d}n_a}{\mathrm{d}t} - \frac{\mathrm{d}n_d}{\mathrm{d}t} - A_{m1} m_1 n_c - A_{m2} m_2 n_c \tag{45}$$

$$\frac{\mathrm{d}n_a}{\mathrm{d}t} = A_a (N_a - n_a) n_c - \gamma_a n_a \tag{46}$$

$$\frac{\mathrm{d}n_d}{\mathrm{d}t} = A_d (N_d - n_d) n_c - f_d n_d \tag{47}$$

$$\frac{dm_1}{dt} = A_{h1}(M_1 - m_1)n_v - A_{m1}m_1 n_c \tag{48}$$

$$\frac{dm_2}{dt} = A_{h2}(M_2 - m_2)n_v - A_{m2}m_2 n_c \tag{49}$$

$$\frac{dn_v}{dt} = R - A_{h1}(M_1 - m_1)n_v - A_{h2}(M_2 - m_2)n_v \tag{52}$$

where R is the rate (m^{-3} s^{-1}) of generation of electron-hole pairs, the respective probabilities; A_{h1} and A_{h2} are for the hole trapping, A_{m1} and A_{m2} for the recombination centres (m^3 s^{-1}) and n_v is the free hole concentration (m^3) in the valence band. M_1 and M_2 are the radiative recombination centres and the non-radiative recombination centres respectively, m_1 and m_2 are the respective concentrations of electrons or holes at these centres. All other terms are defined as in the simple model.

The PTTL is produced by the recombination occurring at the radiative center. At the start of illumination the number of electrons in the shallow traps (n_a) will be less than the number of holes in the radiative center (m). The expected behavior is for the PTTL signal to increase as n_a increases. At longer illumination times, however, n_a may become greater than m_1. The PTTL may now decrease as m_1 decrease and the PTTL intensity may be given by:

$$I_{PTTL} = -\beta\frac{dm}{dT} - \beta A_{m1}m_1 n_c \tag{53}$$

Using the quasi-equilibrium assumption and substitution, n_c can be obtained. Assuming that retrapping into the acceptor trap is slow and that retrapping into the donor trap is the dominant during heating (i.e. during PTTL signal readout), Alexander and McKeever [19] obtained for the integrated PTTL

$$S_{PTTL} = m_{10}[1-(1-\frac{n_{a0}}{m_{20}})^{A_{m1}/A_{m2}}] \tag{54}$$

If recombination into the non-radiative centre is the main mechanism for the production of luminescence then

$$S_{PTTL} = m_{10}[1-(1-\frac{n_{a0}}{N_d - n_{d0}})^{A_{m1}/A_{m2}}] \tag{55}$$

2.2.3 Wavelength Dependence

The wavelength dependence is also an important characteristic of PTTL effects in TLD materials. The PTTL signal as function of the wavelength of illuminating light is introduced via $f_d = \phi(\lambda)\sigma_d(\lambda)$. Assuming deep levels and parabolic bands σ_d is given by

$$\sigma_d = C\sqrt{E_o}\,\frac{(h\nu - E_o)^{3/2}}{h\nu(h\nu - \delta E_o)^2} \tag{56}$$

where C is a constant, hν is the incident photon energy. δ = 1- m_e/m^* is a constant dependent on the free electron mass m_e and the electron effective mass m^*. E_o is the optical ionization energy of the donor traps.

To measure the PTTL wavelength dependence, the usual procedure is to illuminate the material in use for a fixed time at a given wavelength and monitoring how the resulting PTTL signal (S_{PTTL} (λ)) depends on the wavelength. The true wavelength response (i.e. the shape of the cross photo-ionization cross section) can be obtained by taking the initial slope of the S_{PTTL} (t)) curve (Alexander et al. [35]). Therefore, plotting the initial slope of the PTTL (S_{PTTL} (λ)) against wavelength, a curve shape corresponding to the photo-ionization cross section $\sigma(\lambda)$ is obtained.

CHAPTER 3

3 TL AND PTTL IN THE MATERIALS USED IN THIS STUDY

3.1 Introduction

The TL properties of materials have been studied in details and the literature thereof is voluminous (for recent review, see McKeever et al [6]). The study of UV-induced TL mechanisms in various materials has been of wide interest to many researchers [27-33]. Las and Stoebe [28] studied the TL sensitivity and reproducibility in crystals of MgO exposed to ultraviolet radiation. Okuno [29] studied the UV-induced TL in a green variety of fluorite and observed that the PTTL decays after an initial build up if the UV exposure is prolonged. This was explained by assuming simultaneous trapping and detrapping under UV exposure.

The study of the UV-induced PTTL signal has been of interest to many researchers (Colyott et al [16], Oster et al [21], Akselrod and Gorelova, [20], Colyott [25], Bulur et al [17], Sunta [34], Pradhan and Bhatt [36], Kharita et al. [37]). Sunta [34] showed that PTTL of natural CaF_2 exhibits a linear response to low UV irradiation exposure. According to Bulur and Göksu [17] the study of PTTL is one of the sources of information in understanding the luminescence process in the material of interest.

The introduction of single crystal α-Al_2O3: C TL dosimeter (Akselrod et al. [23,24]) opened a new era in TL dosimetry due to its high sensitivity to radiation. The sensitivity of the crystal to gamma radiation was found to be 50 times higher than that of LiF:MgTi with a blue luminescence band at 420nm. According to Walker et al. [26] one potential limitation in the use of this material is its sensitivity to light. Light sensitivity [20,23] in

this material can be explained in three ways: the generation of a TL signal in unirradiated material, light-induced fading of the radiation-induced signal, and phototransfer of charge from deep traps to shallower traps giving rise to PTTL.

The light-induced fading of the material has been studied by a number of researchers [23-26]. The PTTL signal also has been studied in this material by a number of groups [15-17]. Oster et al [21] and Colyott et al [15], studied the excitation spectra of PTTL. It was observed to have a maximum at 280nm and with a weak shoulder near 340nm. Colyott et al [15] studied PTTL of traps unstable below room temperature, that is traps responsible for TL below room temperature. However Akselrod and Gorelova [20], studied the PTTL signal of α-Al_2O3:C above room temperature, at 190°C. Recently, Bulur et al. [17] studied the 190°C PTTL signal from α-Al_2O3:C using blue emitting diodes. It was observed that the deep (donor) traps responsible for PTTL were stable up to 500°C but heating to temperatures greater than 600°C removes the PTTL effect induced by the blue LED suggesting that the traps become thermally unstable at or near 600°C.

Colyott et al. [16] presented the design of a UV-B dosimeter that measures absorbed ultraviolet dose, for a wavelength band centred at 307nm based on the PTTL of α-Al_2O_3:C. By illuminating a previously γ-irradiated sample with UV light a PTTL signal is induced, the intensity of which is proportional to the dose of UV absorbed. Figure 3.1 shows the PTTL signal as a function of dose as obtained by Colyott et al [16]. The dosimeter is known to measure the integrated UV exposure in air or in water ranging from a few minutes to several days of total exposure. In this work however, the purpose is to study the PTTL properties of CaF_2: Cu (unknown origin), MgO and MgO: Cu (both

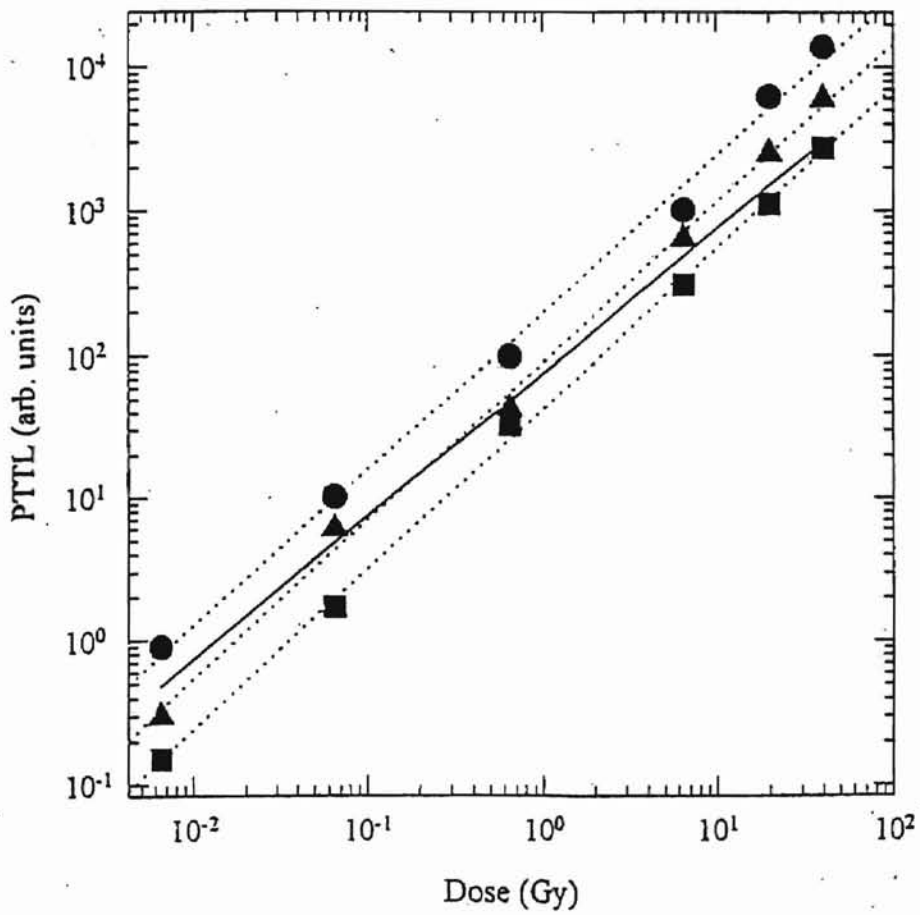

Figure 3.1 PTTL as a function of Absorbed Dose. Absorbed dose of $^{90}Sr/^{90}Y$ delivered at room temperature and heated at 0.3 K s^{-1}. The illumination was at 190 K for 1 min with a photon flux of 6.6 x 10^{14}photon s^{-1} cm^{-2}. Filled circle – 300nm (256K); filled square-500nm (265K); filled triangle – 300nm (450K); full lines –regressions; dashed line-line of linearity.

from ORNL) and to further study the PTTL from α-Al_2O_3:C. The PTTL signal of α-Al_2O_3:C as compared with PTTL from CaF_2:Cu, MgO and MgO:Cu under the same conditions. The study was conducted with the possibility of finding new TL dosimeter materials for UV dosimetry. A detailed study of the wavelength dependence of the materials is also reported, as well as the time dependence of the PTTL signal for fixed wavelength illumination.

3.2 Experimental

The detectors used in the experiments were single chips of α-Al_2O_3:C from LC Technologies, USA, CaF_2:Cu (of unknown origin), MgO:Cu and MgO from Oak Ridge National Laboratory (ORNL). The α-Al_2O_3:C dosimeters were supplied by LC Technologies, in the form of single crystals. The samples were 1mm thick and 5 mm in diameter. The crystals were grown in a highly reducing atmosphere in the presence of carbon under carefully controlled conditions in such a way that high concentrations of F and F^+ centres (approximately $(1\text{-}5)\times10^{17}cm^{-3}$ and $(5\text{-}10)\times10^{15}\ cm^{-3}$, respectively) are produced (Akselrod et. al. [23]). TL emission spectra reveal a broad band centered at 420nm, a characteristic of the de-excitation of excited F centers and emission at 695nm indicating the presence of Cr^{3+} ions of unknown concetration. The dosimeters were annealed at 900°C for 15 minutes before the experiments to release any charges stored in deep traps that might result in TL.

The CaF_2: Cu samples were available in the form of single crystals of diameter 4.86 mm and thickness 0.91mm (measured in our lab). The samples were annealed at 600°C for 1hour. The growth method for the samples was not known.

Both MgO: Cu and MgO dosimeters were prepared ~20 years ago by Dr Yok Chen. These materials were annealed at 1000°C for 3hrs. The annealing procedures for the samples were as recommended in McKeever et al. [6].

Initial irradiations were performed using a ^{60}Co gamma source at room temperature with a dose of 40Gy for each sample. The samples were then heated linearly from 0°C to 500°C, at a linear heating rate of 1°C s^{-1}. The TL for all the samples was measured during heating using the Risø TL/OSL system (Bøtter-Jensen [38-40]). The reader is equipped with a bialkali Thorn EMI 9635QB PMT. During TL readings, no filters were used. An aperture 0.062" (1.588mm) was used in the measurement of the signal. The TL and PTTL measurements were performed in a nitrogen environment. Each sample was purged prior to each measurement for 20s with nitrogen at approximately 10 psi.

To measure the PTTL signal as a function of illumination time, the procedure described above for measuring TL was performed for all the samples. All illuminations were performed with a high irradiance, full spectrum 30 W Deuterium lamp (model 63163). The lamp was operated with an Oriel power supply (model 68940), with a DC output of 300mA. During illumination the samples were placed individually in the UVB dosimeter. Figure 3.2 shows the schematic representation of the UVB dosimeter design. The dosimeter is known to be light tight (i.e. no leakage) and watertight (Colyott et al. [16]). The dosimeter has a 25mm diameter UVB interference filter (CVI model, F25-307.1-4, diameter 25.4mm, thickness 3.5mm) centred at 307nm with a FWHM of 25nm.

Illumination time dependence was performed for all the samples using a 307nm UV light. The pre-irradiation annealing was performed for all the samples as before, followed by dose of 40Gy each. For α-Al_2O_3:C illuminations were performed starting from 3 min

to 6000 min. Due to the low sensitivity signal of the other samples to 307nm UV light, illuminations were performed from 30 min to 6000min.

The wavelength dependence was performed using the same lamp as above. In this case, light from the lamp was focused onto the entrance slit of a 218 GCA McPherson monochromator with 1200 lines mm^{-1} grating with a linear dispersion of 2.65nm mm^{-1}. The wavelength was varied between 250nm to 450nm with 10nm increments. A constant incident photon flux (i.e. average number of photons arriving per unit of time) of 2.5988x 10^{11} s^{-1} cm^{-2} was maintained during the illumination for all measurements by adjusting the power (i.e. by varying exit slit) at each new wavelength. The light power was measured with a Newport Optical Power Meter (model 840) and a Newport silicon photodiode (model 818-UV). The wavelength dependence for all the samples was done following the same procedure of pre-anneal, irradiate, then read TL measurement. After TL measurement, each sample was illuminated for x min with UV light of a given wavelength, then the PTTL signal was read. For each sample the procedure above was repeated for each new measurement. Illumination time for α-Al_2O_3:C was 1min, and was 10min for CaF_2:Cu.

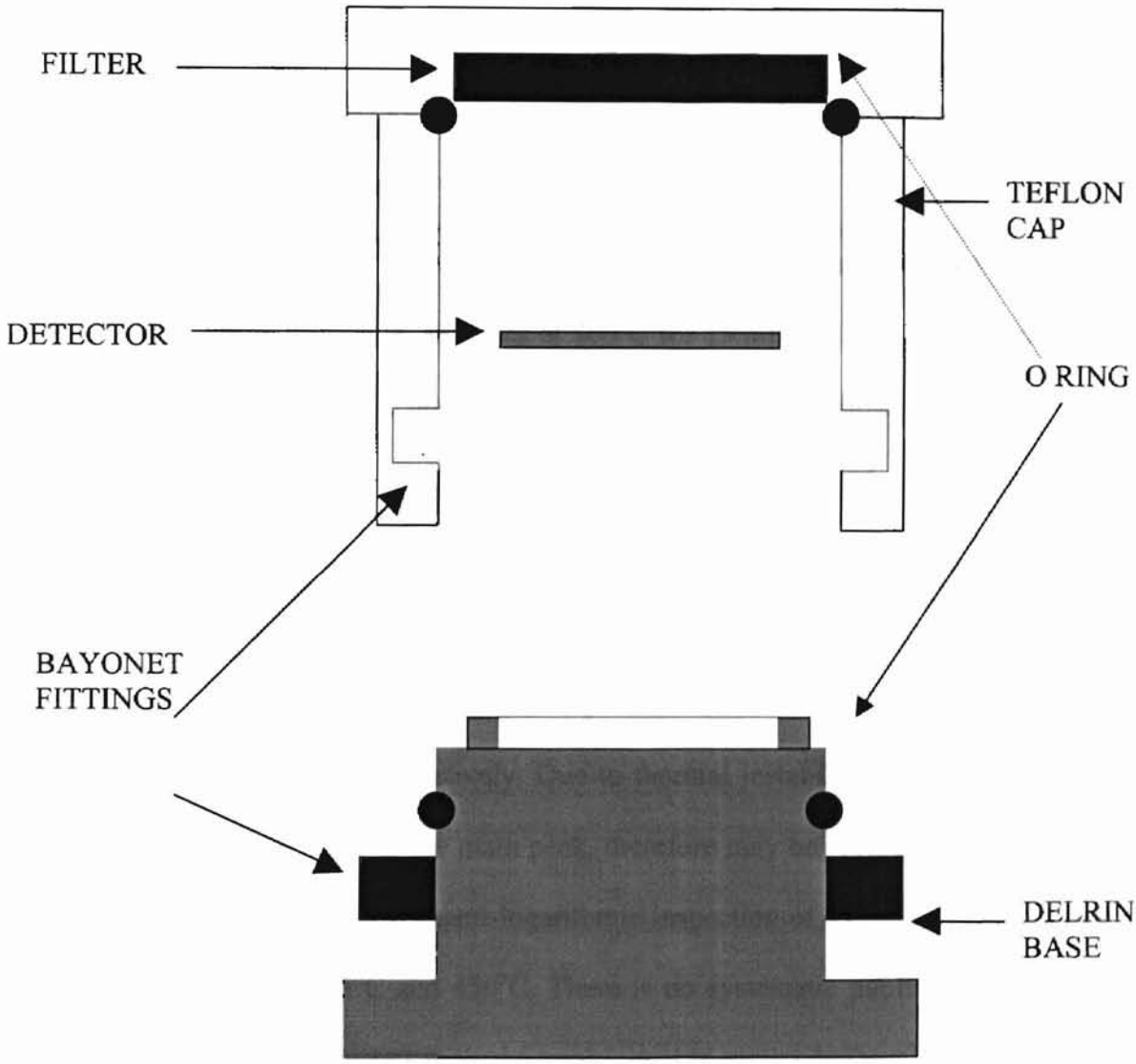

Figure 3.2 Schematic representation of the UVB Dosimeter design. The dosimeter has 25mm diameter UVB interference filter (CVI model, F25-307.1-4, diameter 25.4mm, thickness 3.5mm) centred at 307nm with a FWHM of 25nm.

CHAPTER 4

4 RESULTS AND DISCUSSION

4.1 Results

4.1.1 Thermoluminescence glow peaks

The glow curves from Al_2O_3 show a variety of shapes, dependent upon the impurities and growth conditions. A typical TL glow curve from α-Al_2O_3:C following irradiation of 40Gy ^{60}Co at room temperature and heating at $1^{\circ}C.s^{-1}$ is shown in figure 4.1 (a) and (b). The sample was pre-irradiation annealed at 900°C for 15 min. The data in the linear plot (a) shows the main dosimetric peak at 190°C while the semi-logarithmic plot (b) of same data reflects a complex structure of at least two peaks at ~ 190°C and ~310°C.

Figure 4.2 shows the TL glow curve from CaF_2: Cu irradiated with 40Gy ^{60}Co at room temperature and heated up to 500°C at heating rate $1^{\circ}C\ s^{-1}$. The sample was pre-annealed at 600°C for 1hour. Figure 4.2 (a) shows two peaks, a weak and strong peak (i.e. the main peak) at 100°C and 303°C respectively. Due to thermal instability at low temperatures, the 100°C peak is not taken as the main peak, therefore may be regarded not suitable for dosimetry. Figure 4.2 (b) shows semi-logarithmic inspection of TL with two extra peaks at high temperatures ~385°C and 450°C. There is no systematic published study of the trapping parameters associated with the peaks in this material. Detailed TL peaks are summarized for other CaF_2 doped with Mn, Tm and Dy elsewhere [6]. The 303 peak was fitted using first-order equation. See table 4.1 below for the fitted parameters.

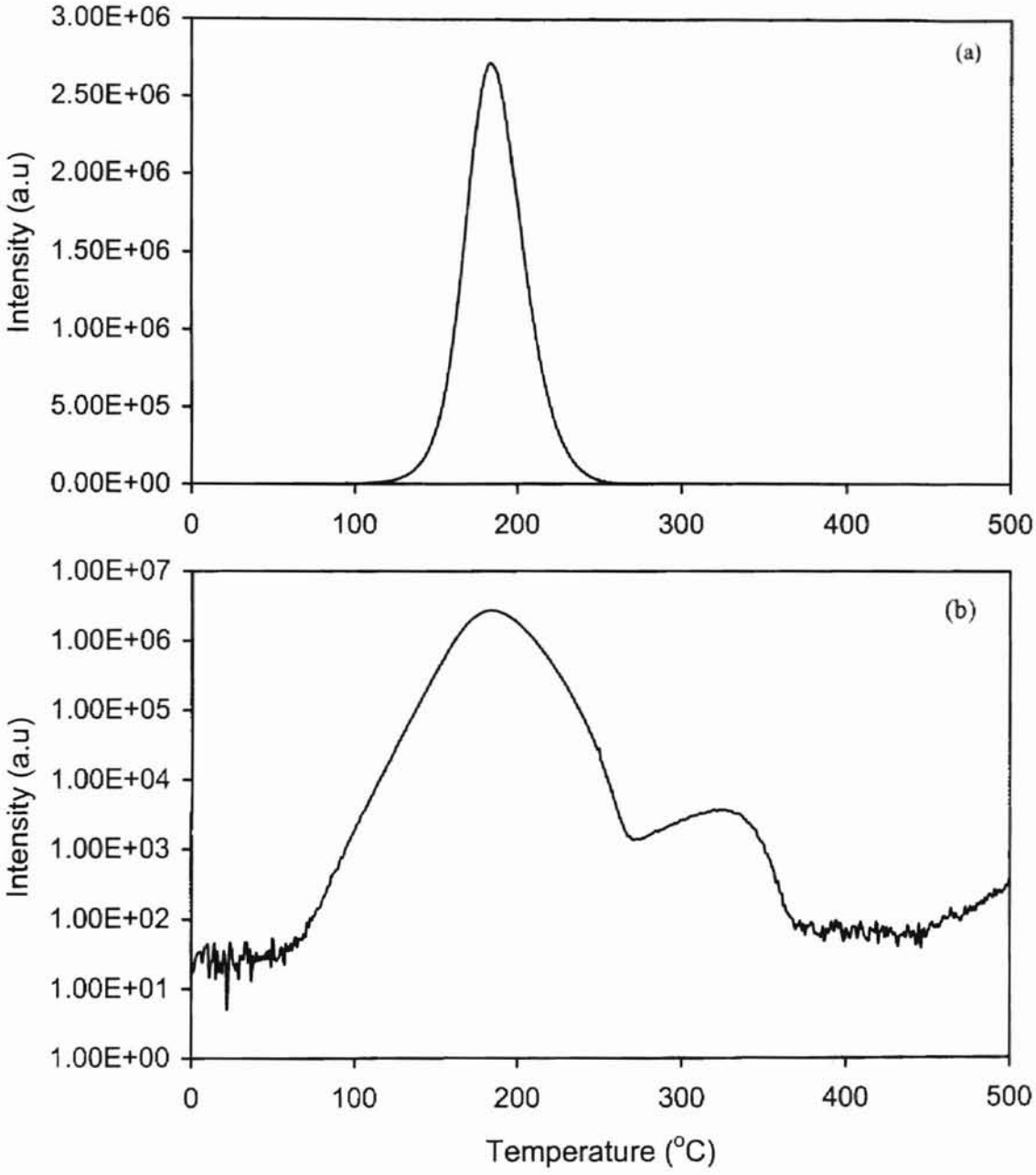

Figure 4.1: (a) TL glow curve for α-Al_2O_3:C following irradiation of 40Gy ^{60}Co at room temperature and heating at $1^{\circ}C.s^{-1}$. The sample was pre-irradiation annealed at 900°C for 15 min. The main peak appears at 185°C. (b) Logarithmic inspection of same data shown in (a)

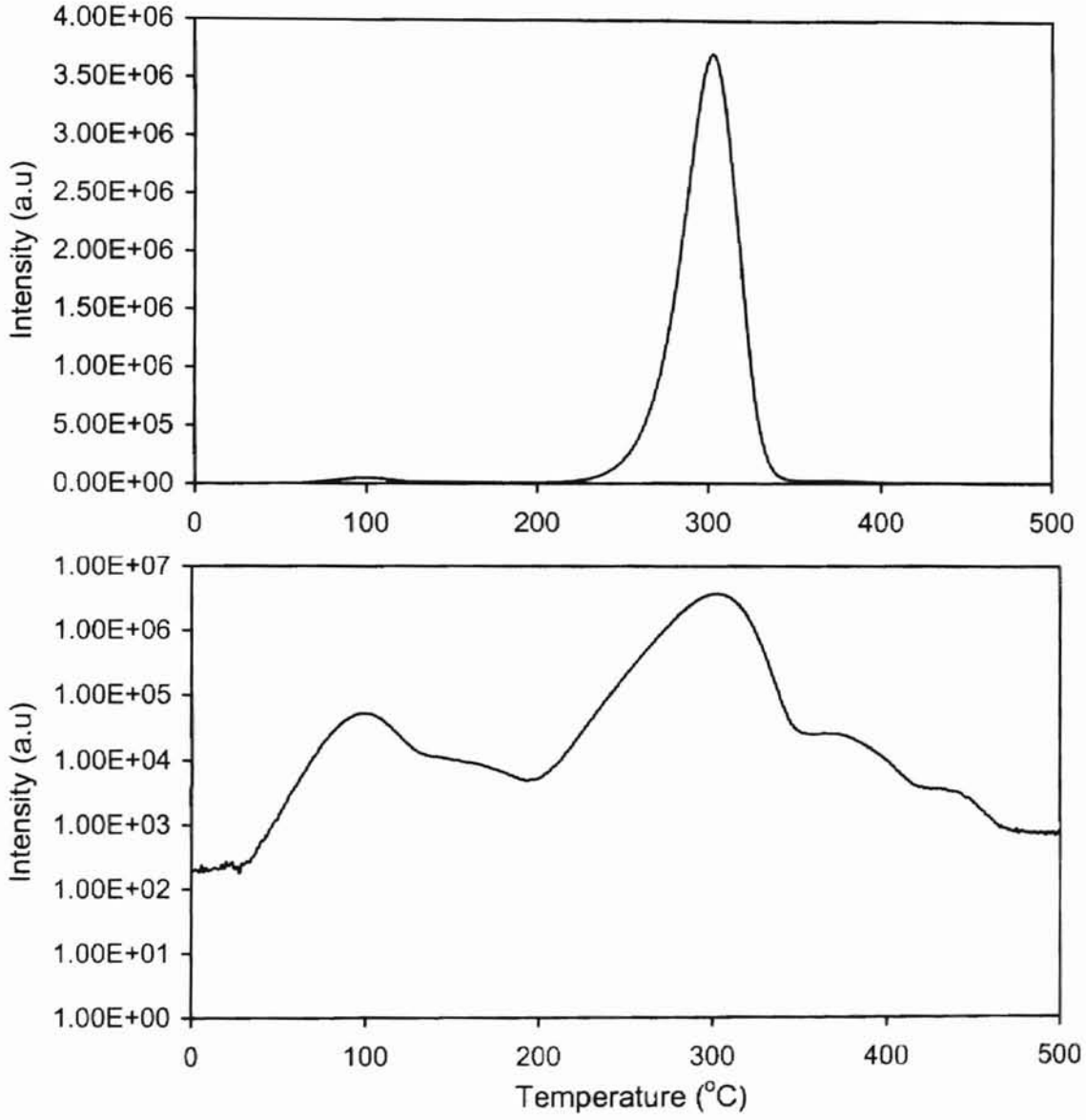

Figure 4.2 (a) TL glow curve for CaF_2: Cu irradiated with 40Gy ^{60}Co at room temperature and heated up to 500°C at heating rate 1°C s^{-1}. The sample was pre-irradiation annealed at 600°C for 15 min. (b) Logarithmic inspection of TL of same as in (a).

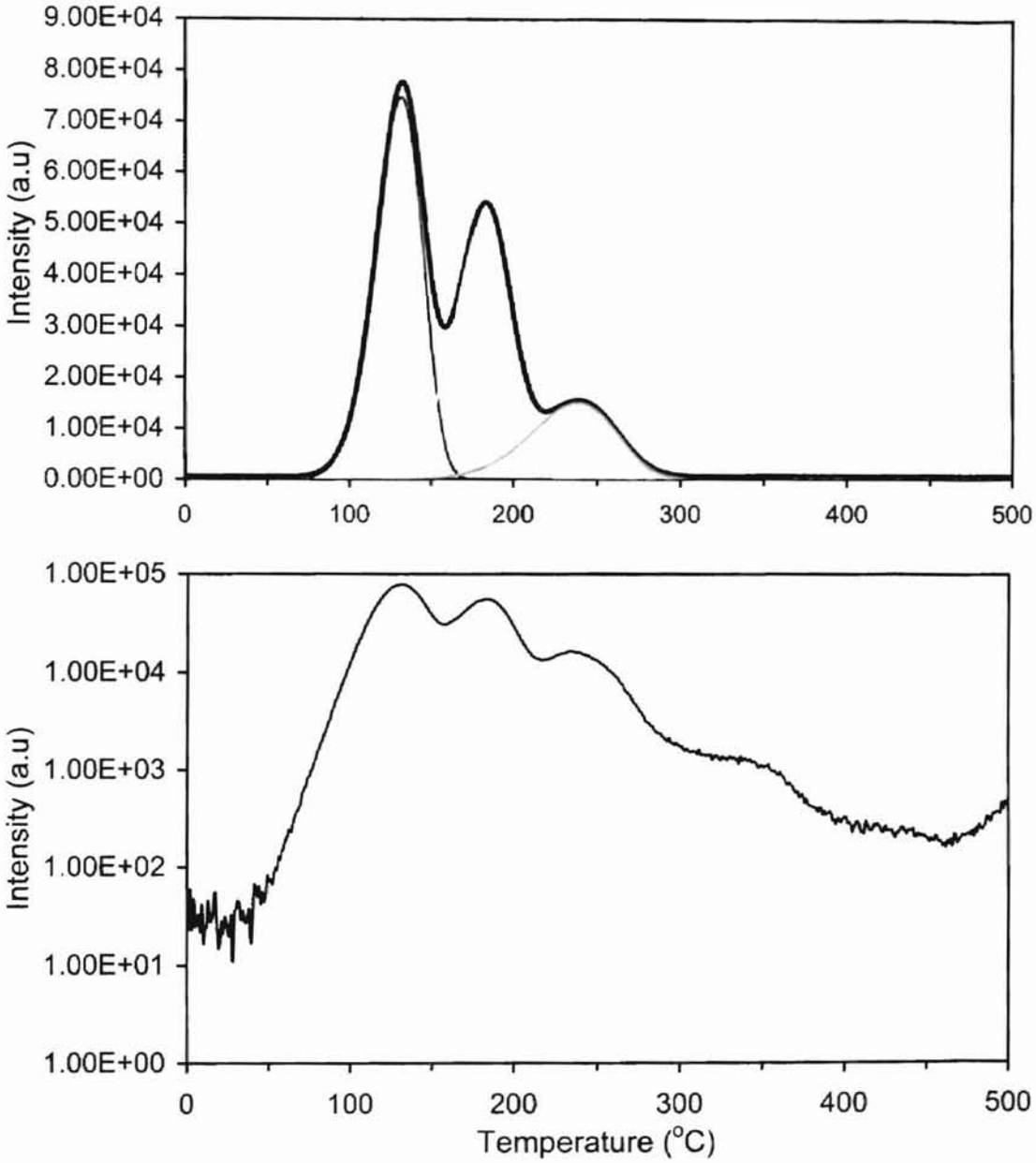

Figure 4.3 (a) TL glow curve for MgO:Cu following irradiation of 40Gy ^{60}Co at room temperature and heating at 1°C.s^{-1} up to 500°C. The sample was pre-irradiation annealed at 1000°C for 3hrs. (b) Shows the logarithmic inspection of the same data as in (a)

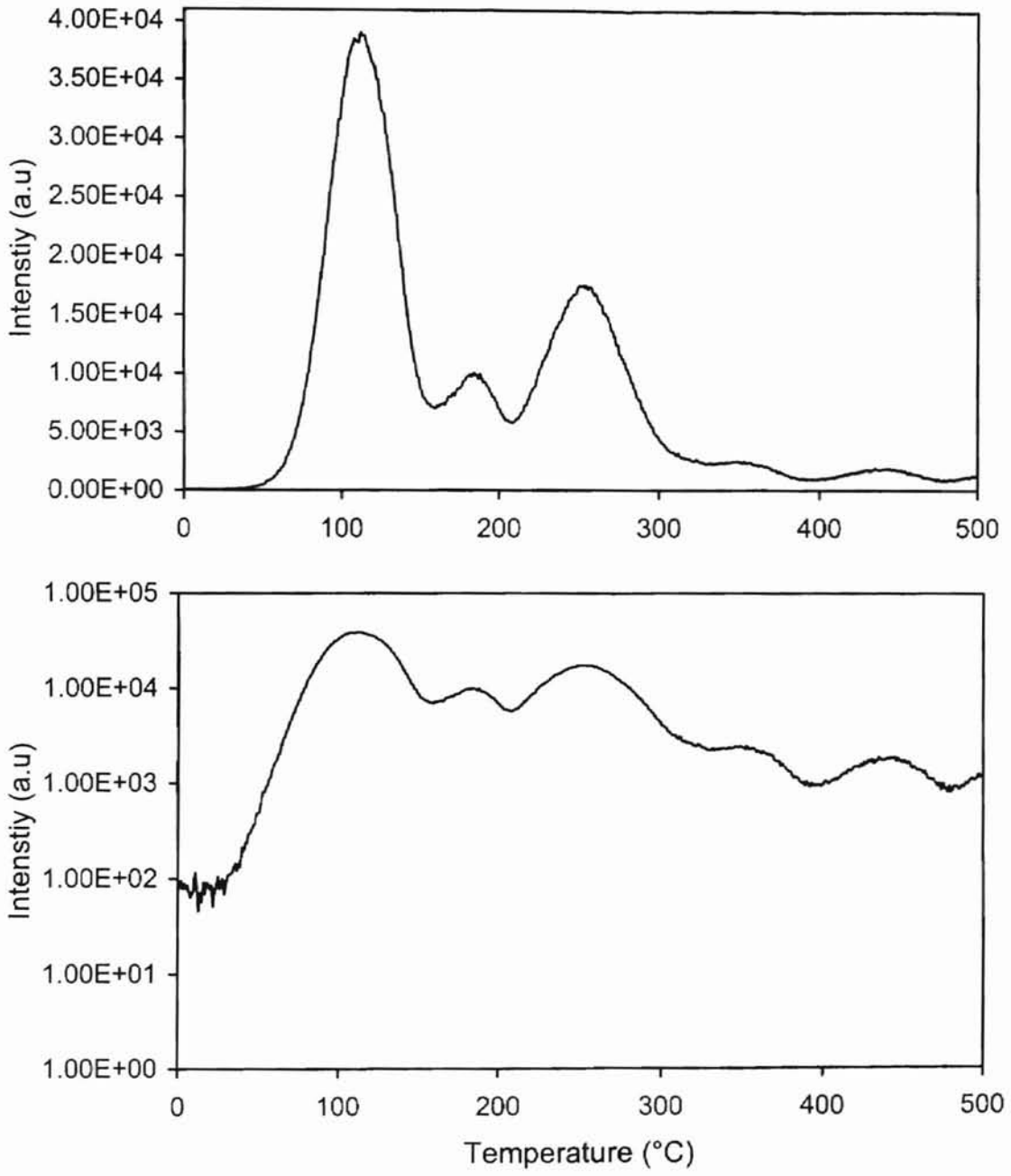

Figure 4.4. (a) Glow curve from MgO following irradiation of 40Gy ^{60}Co at room temperature and heating at $1°C.s^{-1}$ up to 500°C. The sample was pre-irradiation annealed at 1000°C for 3hrs. (b) Shows the logarithmic inspection of the same data as in (a)

Detector	Peak Temperature (^{o}C)	Energy (eV)	Frequency factor s
CaF_2:Cu	303	1.82	5.84×10^{14}
MgO:Cu	130	1.01	3.07×10^{11}
	181	1.0	9.9×10^{9}
	273	0.72	4.51×10^{5}

Table 4.1: Fitted parameters for CaF_2:Cu and MgO:Cu samples. The parameters were obtained by using first-order equations.

In figure 4.3 (a) and (b) the glow curves from MgO:Cu are shown following same irradiation and heating rate as above samples but pre-irradiation annealed at 1000°C for 3hrs. In figure 4.3 (a) peaks are seen to occur at temperatures 130°C, 183°C and 245°C. The semi-logarithmic figure (b) shows the same three peaks, with extra two peaks at ~350°C, ~420°C and an increasing background which maybe a tail of a signal located at higher temperature. The multiple peaks indicate the presence of several trapping species. The TL glow curve was fitted using the first-order equation. See table 4.1 for the fitted parameters of the peaks.

The TL glow curve from MgO pre-irradiation annealed at 1000°C for 3hrs, followed by 40Gy dose of 40Gy ^{60}Co is shown in figure 4.4 (a) and (b). Both figures (a) linear plot and (b) semi-logarithmic plot shows a complex of peaks at 120°C, 195°C, 270°C and two high temperature peaks at ~373°C and ~465°C. An attempt was made to fit the peak using first-order equations but the fit was not particularly good. A better fit was obtained by addition of a single peak to the first peak and another one at the third peak. But such evaluated parameters were not reliable and inconsistent.

4.1.2 Phototransfer Thermoluminescence

PTTL is observed after the crystal is exposed to UV light following irradiation and pre-heating. Figure 4.5. show a typical PTTL signal for α-Al_2O_3:C. After the depletion of the TL signal by heating to 500°C at 1°C, the sample was illuminated with 307nm UVB light. The same procedure was followed for 3min to 6000min illumination time. The PTTL shown in figure 4.5 was obtained after 100 minutes of illumination time. The glow curve has a peak at ~197°C.

Figure 4.6 shows the PTTL signal for CaF_2:Cu. TL was measured before PTTL following an irradiation of 40Gy at room temperature and heating at $1^{o}C.s^{-1}$. The sample was pre-irradiation annealed at 600°C for 1hr. The graph shows the PTTL signal after 100min of UVB illumination. The peak appears at ~303°C.

The PTTL glow curve for MgO:Cu. is shown in figure 4.7. TL was measured before PTTL following an irradiation of 40Gy at room temperature and heating at $1^{o}C.s^{-1}$. The sample was pre-irradiation annealed at 1000°C for 3hr. PTTL shown in figure is for 100 min and 100hrs UVB illumination. As illumination proceeds the shape of PTTL signal resemble those of TL. This suggests that the traps responsible for their productions are the same. In the figure (a) shows the linear plot at ~ 130°C, 183°C and ~245°C and (b) shows the same peaks and high temperature peak at ~350°C covered in the background. It also an increasing background suspected to be the tail of the 420°C and other higher temperature peaks.

Figure 4.8 shows the PTTL glow curve for MgO. The procedure to perform TL measurement was same as before. That is, sample irradiated 40Gy at room temperature and then heated at $1^{o}C.s^{-1}$ up to 500°C. The sample was pre-irradiation annealed at 1000°C for 3hr. PTTL shown in figure is for 100 min and 100hrs UVB illumination. Similar peaks as in TL are observed. The higher temperature peaks seen in the PTTL signals between 30 to 6000min decreased with an increase in the peaks at lower temperatures. This suggests that the depletion of the higher temperature traps correspond to the filling of low temperature traps. A shift to lower temperatures is seen to occur at higher illumination (i.e as the peak grows). This suggest that the glow peaks exhibit

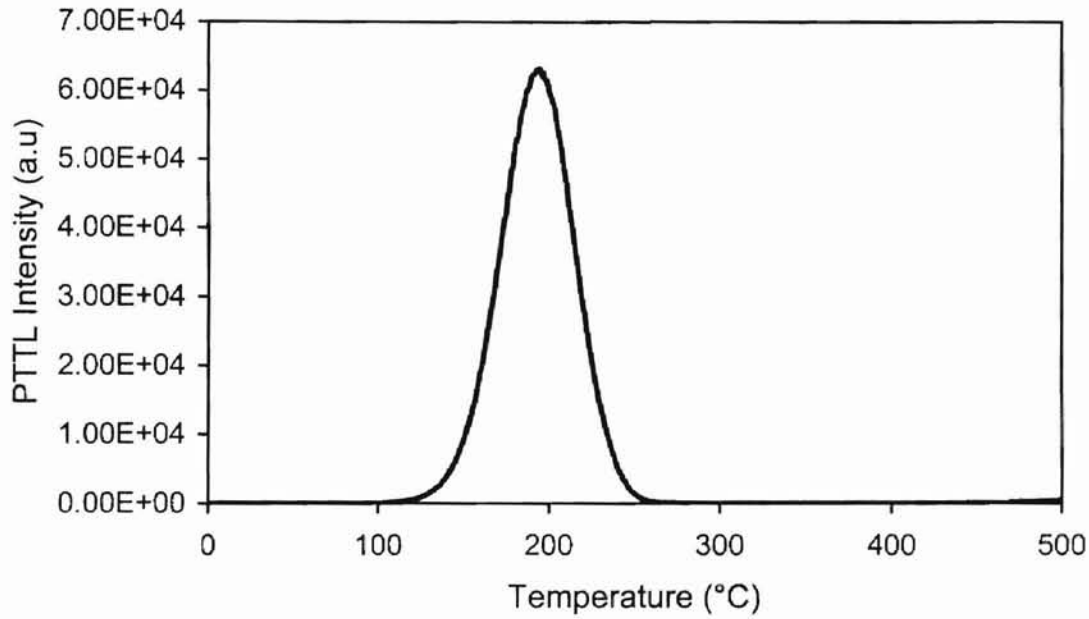

Figure 4.5. PTTL intensity as function of temperature for α-Al_2O_3:C. TL was measured before PTTL following an irradiation of 40Gy at room temperature and heating at $1^{o}C.s^{-1}$. The sample was pre-irradiation annealed at 900°C for 15 min. UVB illumination time 100min. The peak appears at 197°C.

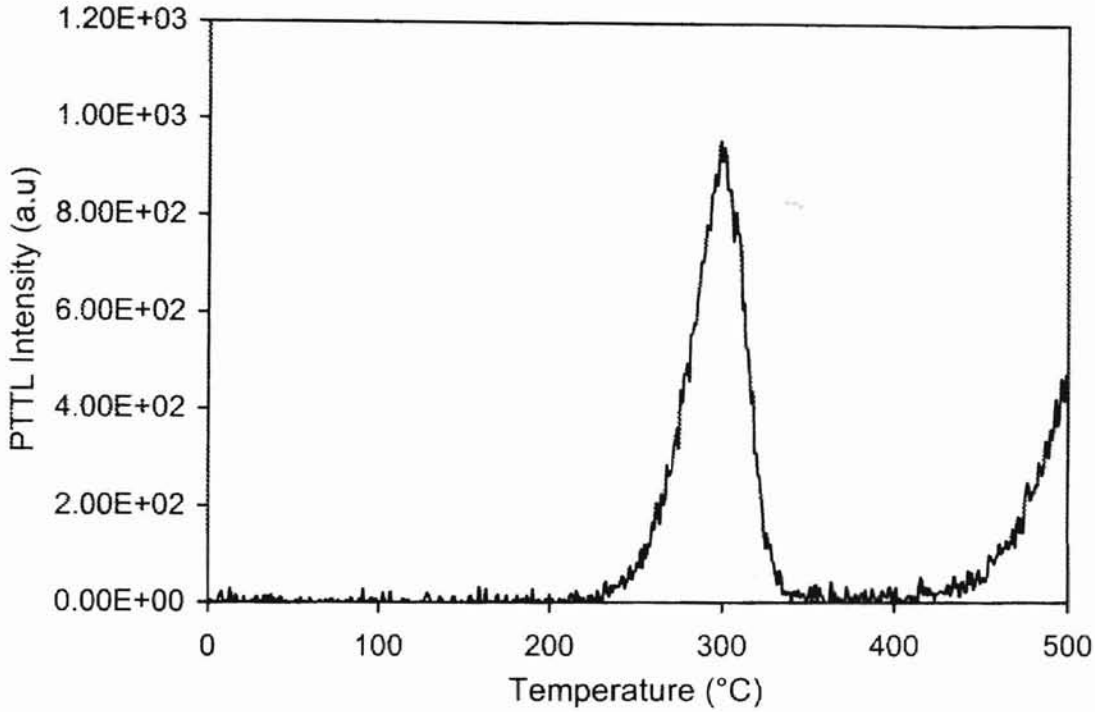

Figure 4.6 PTTL as glow curve for CaF_2:Cu. TL was measured before PTTL following an irradiation of 40Gy at room temperature and heating at $1^{\circ}C.s^{-1}$. The sample was pre-irradiation annealed at 600°C for 1hr. UVB illumination time 100min. The peak appears at ~303°C.

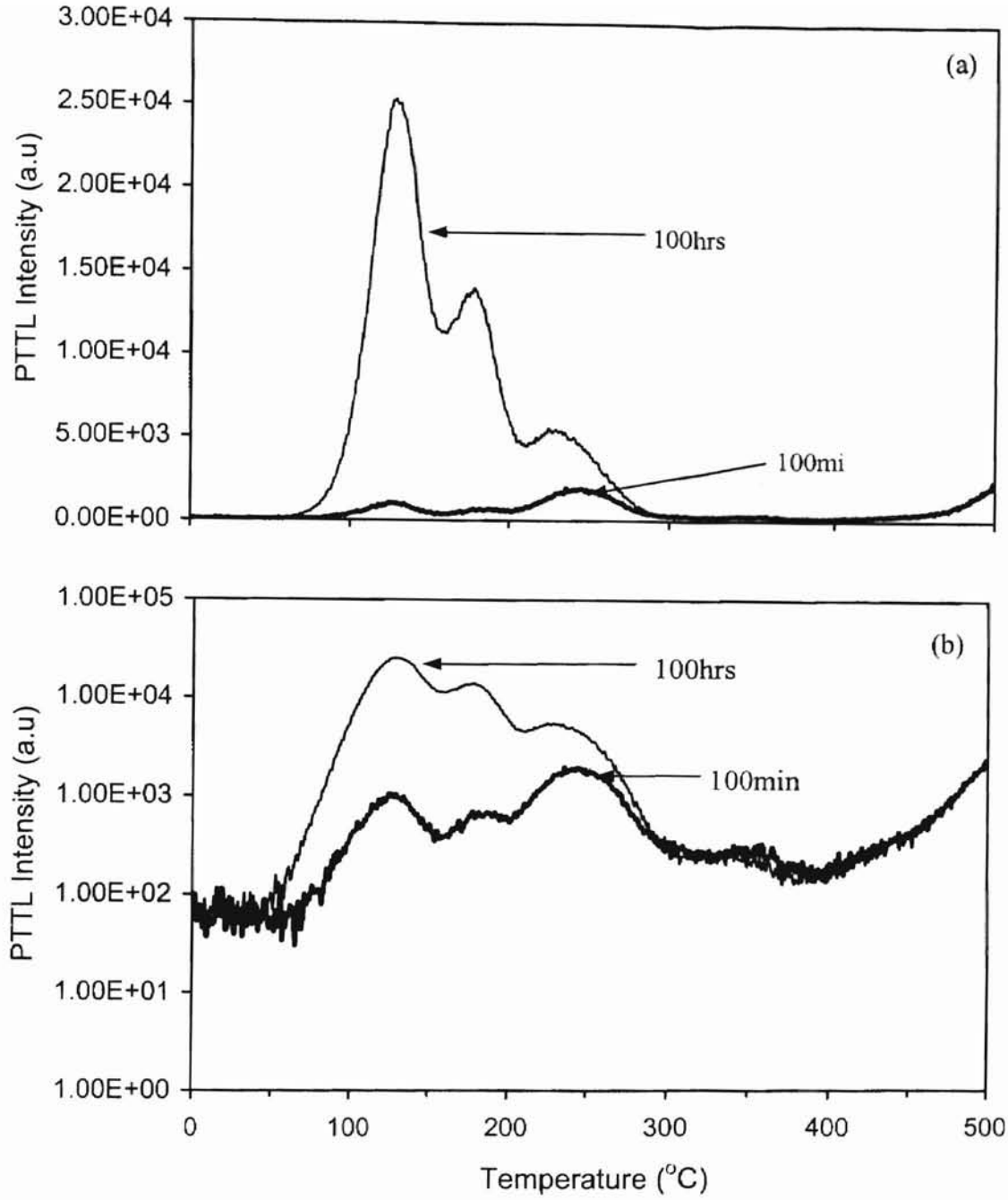

Figure 4.7. PTTL glow curve for MgO:Cu. TL was measured before PTTL following an irradiation of 40Gy at room temperature and heating at $1^{o}C.s^{-1}$. The sample was pre-irradiation annealed at 1000°C for 3hr. UVB illumination time 100min. (a) shows the linear plot and (b) semi-logarithmic plot of same data as (a). PTTL signal shown is for 100min and 100hrs illumination times.

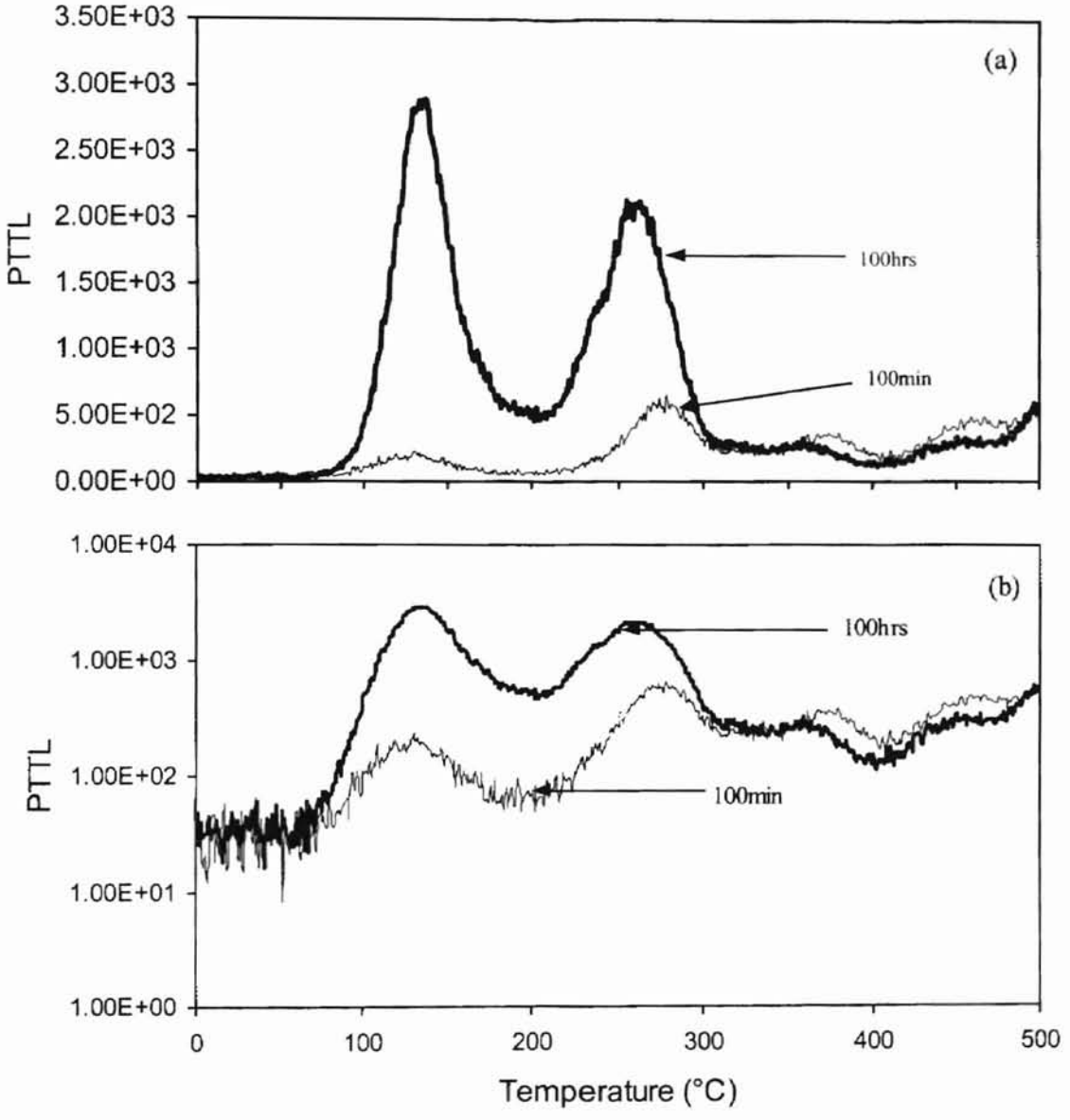

Figure 4.8 PTTL glow curve for MgO. TL was measured before PTTL following an irradiation of 40Gy at room temperature and heating at $1°C.s^{-1}$. The sample was pre-irradiation annealed at 1000°C for 3hr. UVB illumination time 100min. (a) shows the linear plot and (b) semi-logarithmic plot of same data as (a). PTTL signal shown is for 100min and 100hrs illumination times.

second-order behaviour. This might be supported by failure to fit TL glow curve using first-order equation.

Discussed below are the results of the PTTL against illumination time for crystals used in the study. The relative time range used is sufficient to test the PTTL theory of the previous chapters. The PTTL signal used for study is the area under the so called "dosimetry peak".

A typical time response curve for a PTTL signal is shown in Fig. 4.9 for Al_2O_3:C irradiated with 40Gy ^{60}Co at room temperature and pre-heated up to 500°C at heating rate of $1^{\circ}Cs^{-1}$. In the figure, (a) shows the time interval from 3 to 6000min (100hrs) and (b) shows time from 3 to 100 min of UV light exposure at 307nm wavelength. Figure (a) is characterized by an increase followed by a decrease in the PTTL signal. The graph suggests a competition for charge in the dosimetry trap, an increase of charge due to phototransfer from deep trap and photo-stimulated decay of charge out of the dosimetry trap at the same time. The graph starts decaying after reaching a maximum at 1000min. Even though the PTTL has not reached zero after 100hrs of UVB illumination exposure, we know in this case that there is simultaneous optical emptying of charge out of the dosimetry trap. This is supported by getting OSL and photoconductivity by optically emptying the charge from the dosimetry trap. Such results were reported by Whitley and McKeever [41]. Therefore PTTL signal is expected to eventually reach zero after a long illumination time. For a PTTL signal which shows a decrease in the PTTL level to zero, Wintle and Murray [22] argue that this is caused by simultaneous optical detrapping of the charge from the PTTL traps. However, Alexander and McKeever [18] argue that, for

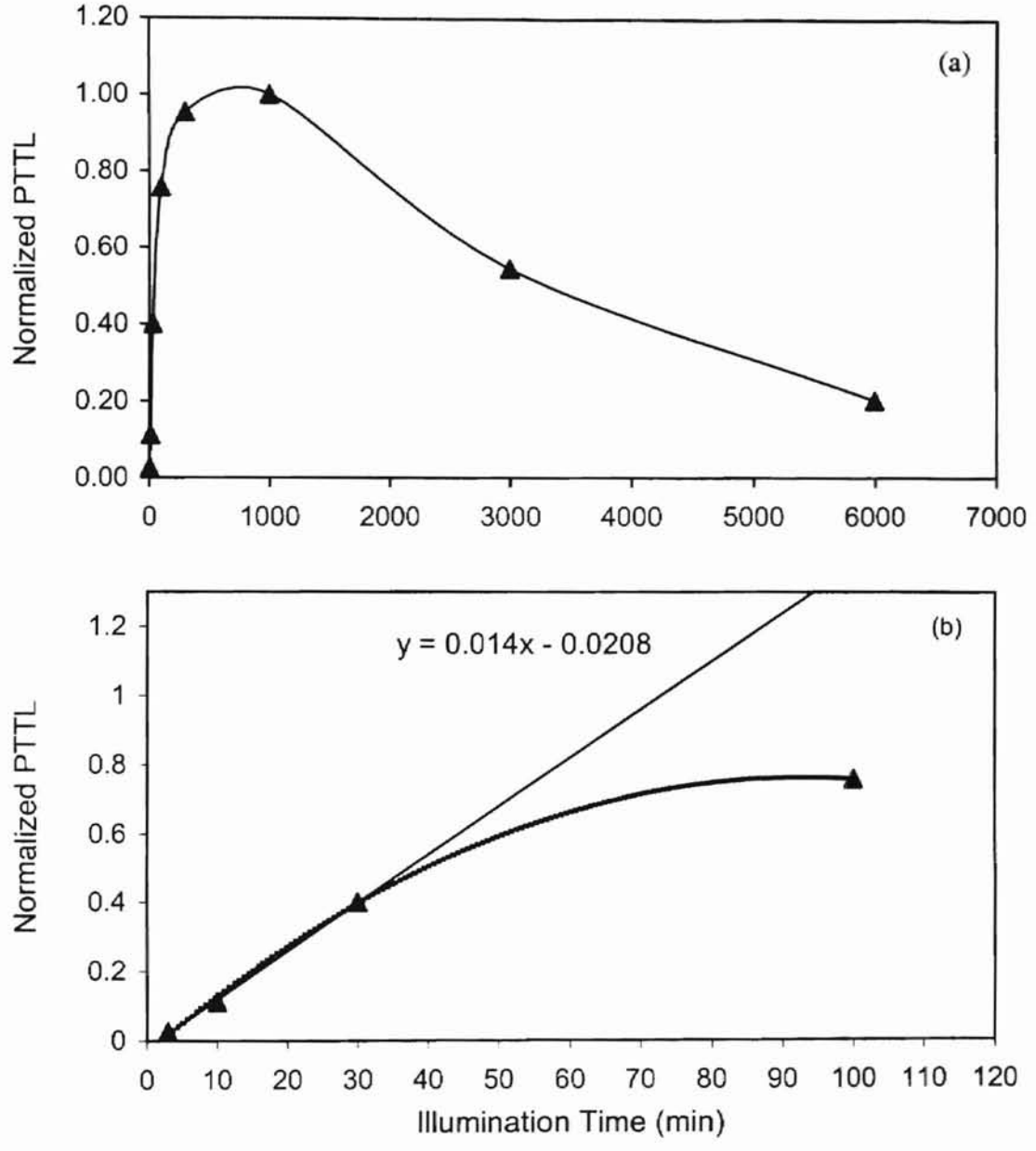

Figure 4.9. PTTL signal (integration region: 130-260°C) as a function of illumination time for α-Al_2O_3:C irradiated with 40Gy ^{60}Co at room temperature and heated up to 500C at heating rate of 1Cs. (a) shows the time interval 3 to 6000min, (b) shows time from 3 min up to 100 min of UV light exposure for the 307nm wavelength.

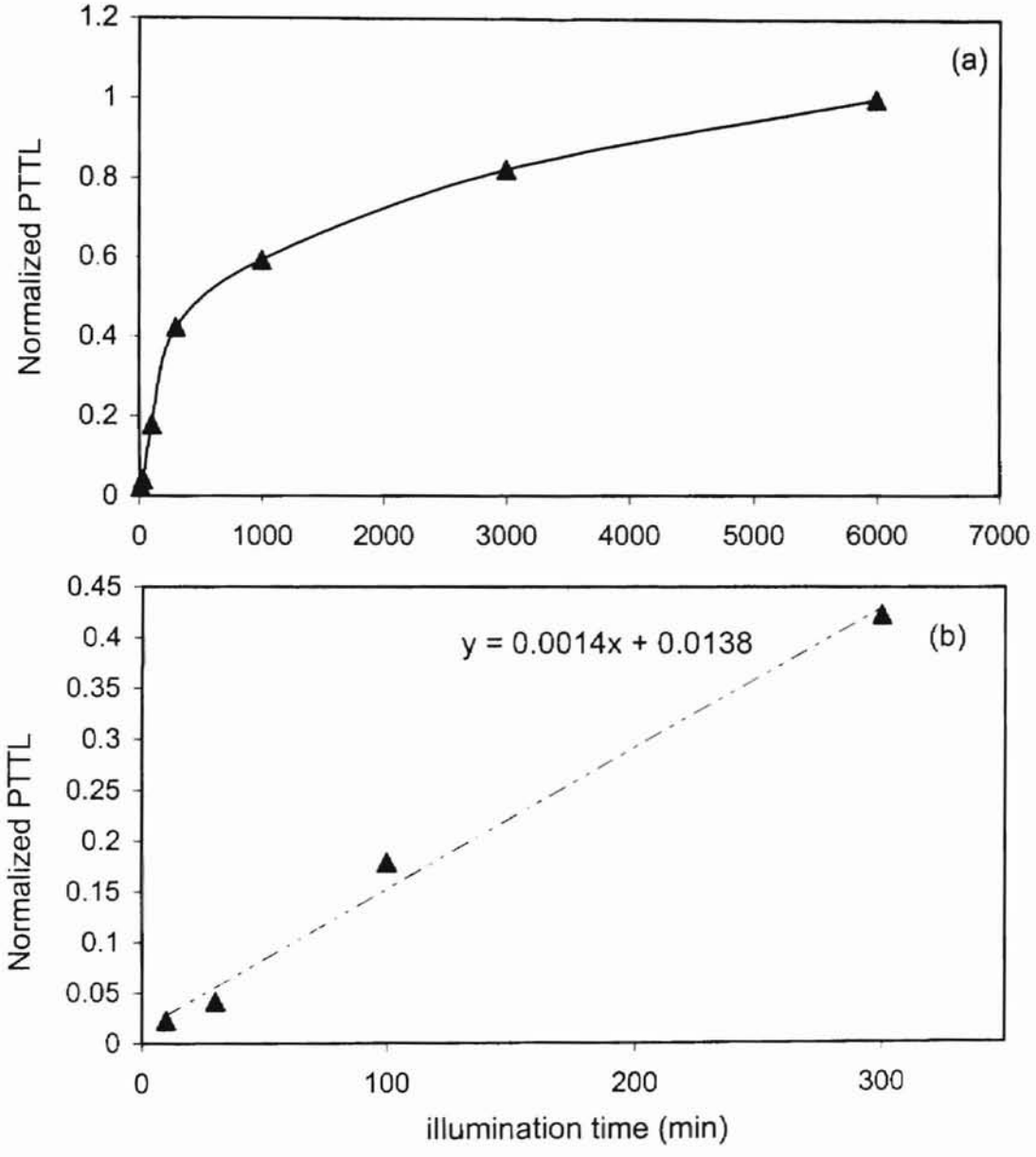

Figure 4.10 (a) PTTL intensity (integration region: 230-330°C) as a function of illumination time for CaF_2:Cu. At each point, after the PTTL measurement, the dosimeter was annealed at 600°C for 1hr, re-irradiated with 40Gy ^{60}Co at room temperature then read TL at a heating rate 1°C s^{-1}. (b) shows time of illumination from 10 min to 300 min.

those PTTL signals that decrease after long illumination time but do not reach zero level, the decrease in such peak could not be caused by the simultaneous optical emptying of the PTTL traps during phototransfer. At least in such cases the complex model of chapter 2 can be used to describe the behavior of the PTTL signal. Figure 4.9(b), show some nearly linear PTTL response at low illumination times, therefore UV light in this region of time can be used for dose reassessment.

In figure 4.10(a) the PTTL intensity (integration region: 230-330°C) as a function of illumination time for CaF_2:Cu is displayed. At each point, after the PTTL measurement, the dosimeter was annealed at 600°C for 1hr, re-irradiated with 40Gy ^{60}Co at room temperature then the TL was read at heating rate 1°C s^{-1}. The behavior of the PTTL signal is seen to increase monotonically with time. Few conclusions can be drawn from the behavior of this graph. However, at this point the graph tells that there is no optical excitation from the acceptor traps during illumination and no equilibrium has been reached. Therefore it might be expected that after very long illuminations PTTL signal might reach steady state level (i.e. a point were donor traps are depleted). On the other hand, the graph might start decreasing and reach a zero level if optical excitation out of the acceptor trap is possible. Hence the fundamental different behaviors can be expected from this material. Figure 4.10(b) shows an extrapolation of the linear behaviour of the PTTL time curve as an approximation for very short illumination time.

The sensitivity of MgO and MgO:Cu samples were too small at low UV illumination times such that the PTTL output could not be distinguished from the background signal. As a result the PTTL measurements were started after 30min illuminations. Illuminations were performed with a 307nm UV light as in the other materials.

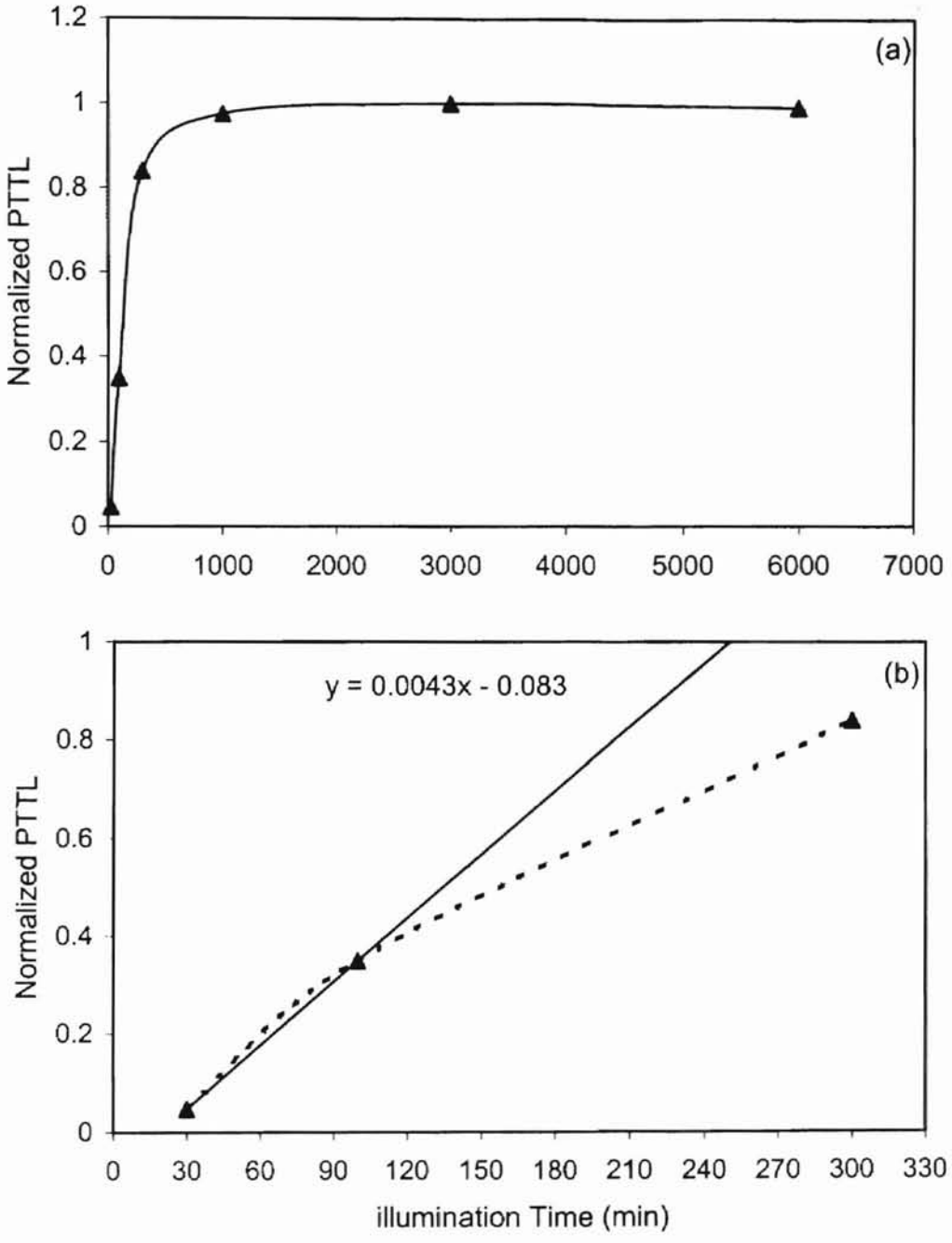

Figure 4.11 PTTL peak height as function of illumination time for MgO:Cu. At each point, after the PTTL measurement, the dosimeter was annealed at 1000°C for 3hrs, re-irradiated with 40Gy ^{60}Co at room temperature then read TL at a heating rate 1°C s^{-1}. (a) show the time interval from 30 to 6000 min and (b) the time interval from 30 to 1000 min.

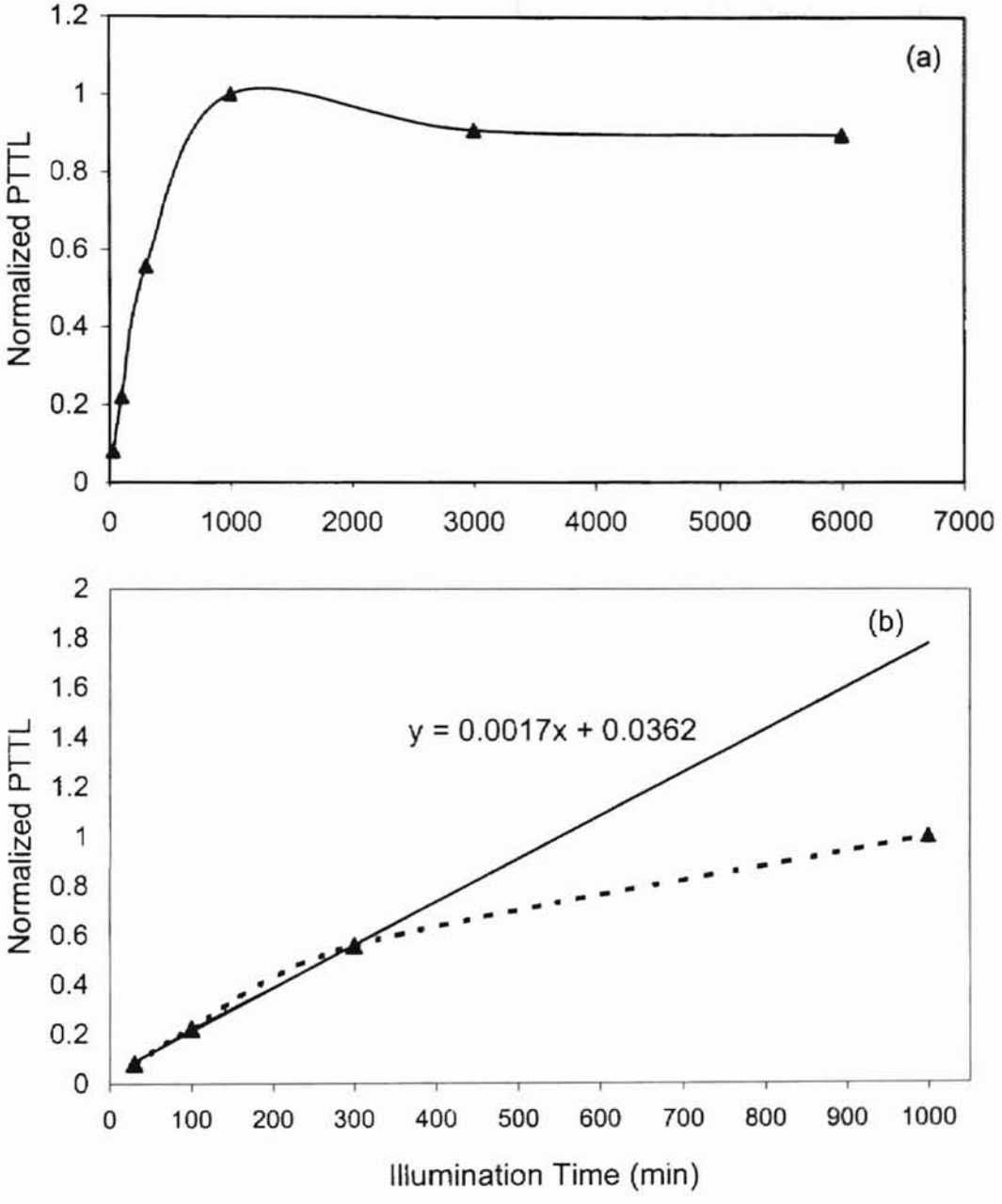

Figure 4.12. PTTL intensity (integration region: 210-310°C) as a function of illumination time for MgO. At each point, after the PTTL measurement, the dosimeter was annealed at 1000°C for 3hrs, re-irradiated with 40Gy ^{60}Co at room temperature then read TL at a heating rate 1°C s^{-1}. (a) show the time interval from 30 to 6000 min and (b) the time interval from 30 to 1000 min.

The PTTL peak height as function of illumination time for MgO:Cu is shown by figure 4.11. The dosimeter was annealed at 1000°C for 3hrs after every PTTL measurement. At each point, after the PTTL measurement, the dosimeter was annealed at 1000°C for 3hrs, re-irradiated with 40Gy ^{60}Co at room temperature then read TL at a heating rate 1°C s^{-1}. In the figure (a) show the time interval from 30 to 6000 min and (b) the time interval from 30 to 1000 min. Figure 4.11 (a) shows a monotonically increasing behaviour in the PTTL signal as function of illumination time up to a steady-state saturation level. The PTTL signal shows saturation in the intensity at ~1000 min of UVB exposure for the ~245°C peak. This was not the case with the other peaks (i.e. ~130°C and ~183°C) at this illumination time. These peaks were seen to increase even after long illumination time. However all the peaks suggests no optical excitation out of the shallow trap during UV illumination.

Figure 4.12 shows the PTTL intensity (integration region: 210-310°C) as a function of illumination time for MgO. The same procedure used for in MgO:Cu sample was followed. In attempt to explain the behaviour of this graph, the same models of Alexander et al. [19] were adopted. In figure (a) the characteristic is that of an increase in the signal followed by a decrease to some high steady-state level. The decrease is observed after 1000min. No appreciable change in the PTTL was observed after 3000min, an implication that the PTTL peak cannot be losing charge due to optical excitation. The same behaviour in the PTTL was observed using the peak height. Figure 4.12(b) shows illuminations from 30 min to 300min.

In order to understand emptying of the donor traps, i.e. the decay behavior of the PTTL signal with re-use, PTTL from all the samples were monitored successively by

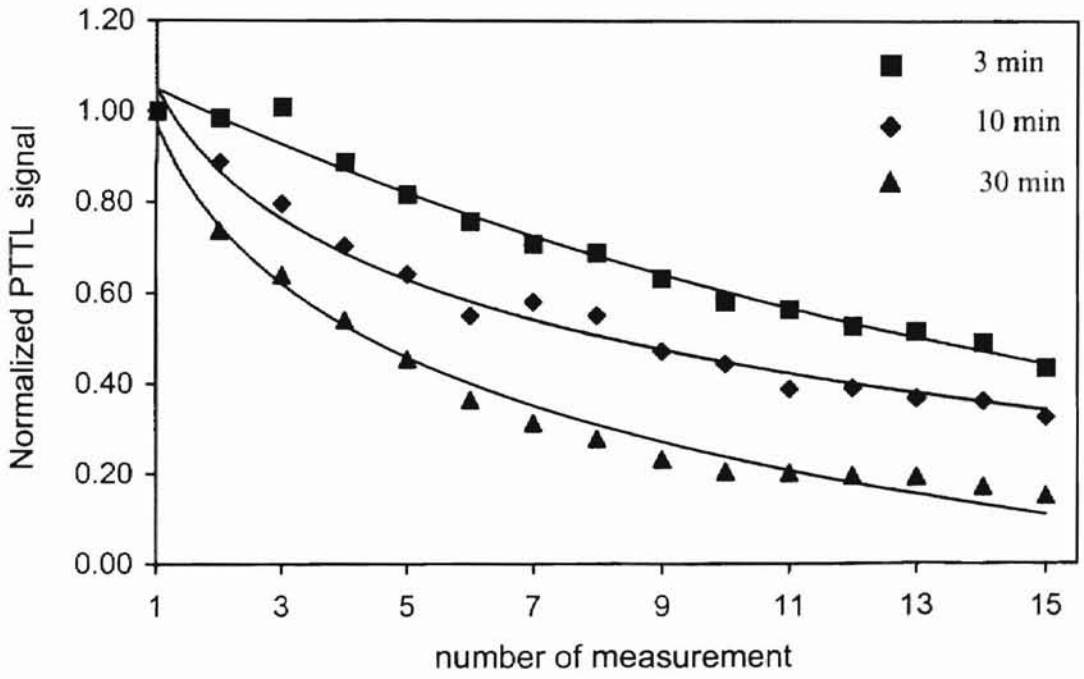

Figure 4.13. The decay of the PTTL signal (integration region 130°C-260°C) as a function of re-use for various illumination times for α-Al_2O_3:C. The sample was irradiated with 40Gy ^{60}Co dose and heated during TL readout at $1^{\circ}Cs^{-1}$ up to 500°C. PTTL was measured by successive illuminations.

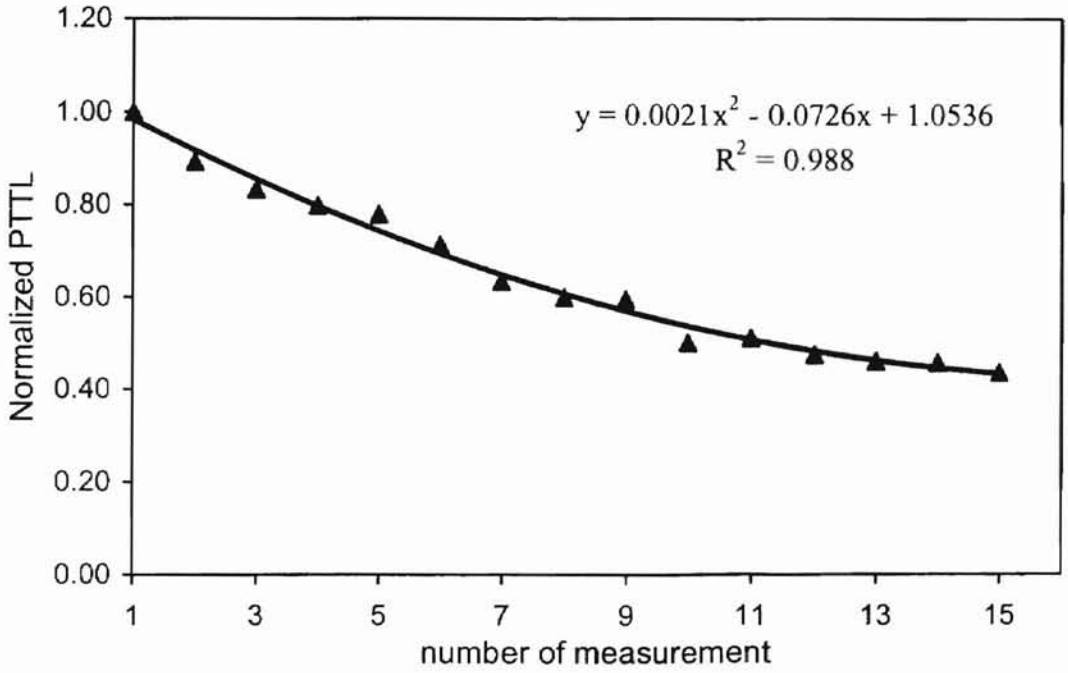

Figure 4.14 The PTTL decay of CaF_2:Cu (integration region 230°C-330°C) against re-use for the 30 min UV illumination. Irradiation dose 40Gy ^{60}Co at room temperature and pre-irradiation annealed at 600°C for 1hr. PTTL was measured by subsequent illuminations.

repeatedly illuminating the samples and measuring the thermoluminescence. After the TL measurement, each sample was illuminated for 1hr with UV light of wavelength 307nm then PTTL was measured. To obtain the decay, further illuminations were performed for each sample without re-annealing the samples.

Figure 4.13 shows the decay of the normalized PTTL signals obtained with 3, 10 and 30 min illumination time as a function of re-use for α-Al_2O_3:C. The sample was irradiated with 40Gy ^{60}Co dose and heated during TL readout at $1^{o}Cs^{-1}$ up to 500°C. Subsequent illuminations were performed without re-annealing the sample after each TL measurement. As seen from the figure the rate of emptying of traps becomes faster with an increase in illumination time. This is supported by the 30min graph showing a faster decaying behaviour than both the 3min and the 10min graphs. The readings of the PTTL output shows a decay behavior shown by the extrapolation curve. The 3min illumination curve shows exponential decay behavior.

Figure 4.14 shows the normalized PTTL decay signal for CaF_2:Cu (integration region 230°C-330°C) subjected to severe 30min illuminations of 307nm light. The sample was a 40Gy given dose and pre-annealed as before. PTTL was measured for subsequent illuminations. The line reflects the rate at which deep traps are emptied by the incident photons.

Figure 4.15 shows the decay of PTTL signal (integration range 220°C-320°C) for MgO:Cu against number of measurements for 30 min UV illumination at 307nm. The irradiation dose was 40Gy ^{60}Co at room temperature and the sample was pre-irradiation annealed at 1000°C for 3hrs. The curve shows a quick decay of ~40% between the first and the third peak then starts to decay slowly with further illumination.

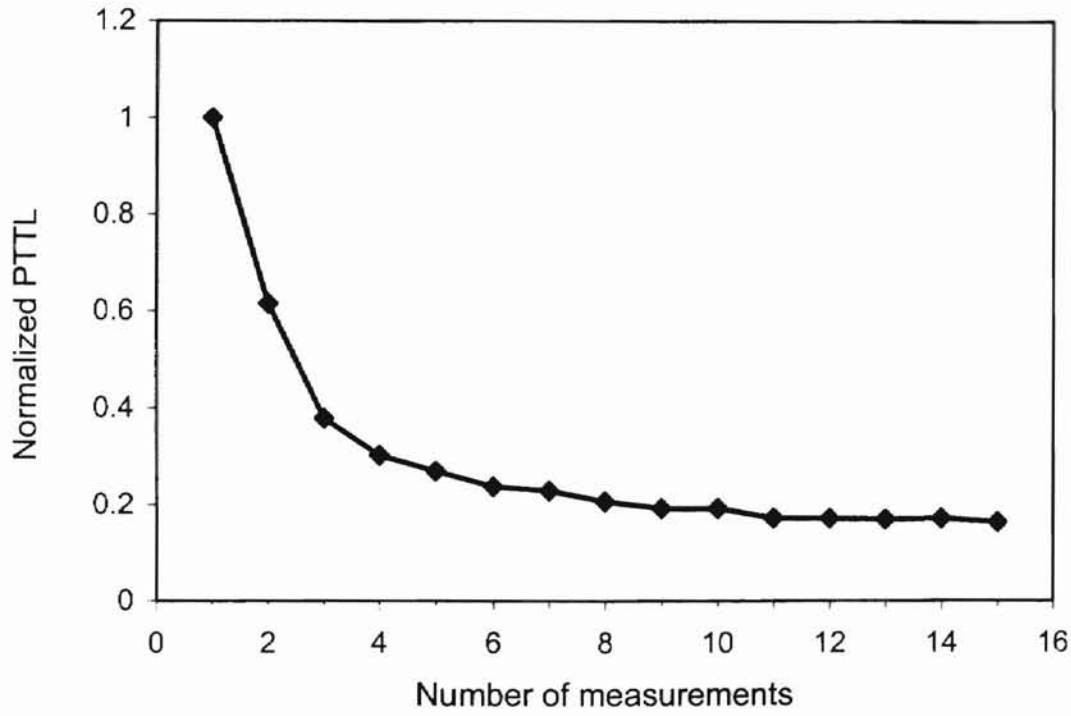

Figure 4.15: The decay of PTTL signal (integration range 220°C-320°C) for MgO:Cu against number of measurements for 30min UV illumination at 307nm. Irradiation dose 40Gy ^{60}Co at room temperature and pre-irradiation annealed at 1000°C for 3hrs.

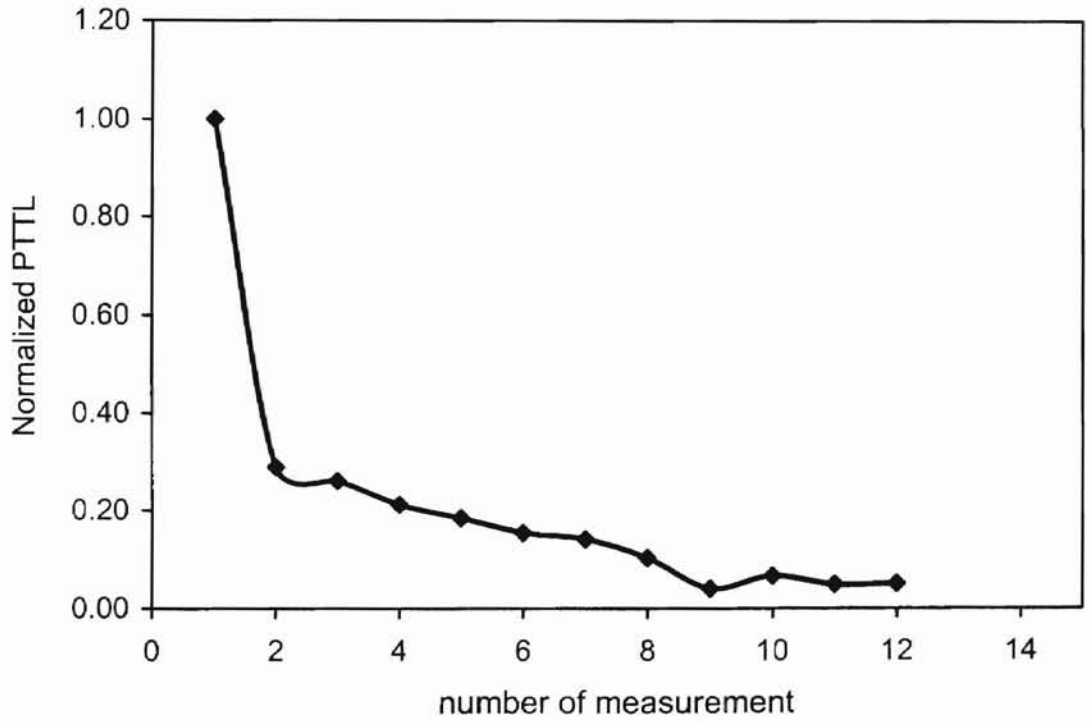

Figure 4.16 The decay of PTTL signal (integration range 210°C-310°C) for MgO against number of measurements for 30min UV illumination at 307nm. Irradiation dose 40Gy ^{60}Co at room temperature and pre-irradiation annealed at 1000°C for 3hrs.

Figure 4.16 shows the PTTL signal for MgO as a function of re-use for 30min UV illumination, also at 307nm. The sample was dosed and pre-annealed as before. The curve shows a quick decay to ~28% of its initial value, then starts to decay slowly with illumination.

4.1.3 Wavelength Dependence

The effect of the stimulation wavelength on the PTTL response was also studied. Usually the wavelength dependence for the phototransfer involved the method of arbitrarily selecting a given illumination time and monitoring the PTTL intensity at that time for a given wavelength [41]. However, the wavelength dependence obtained in such a manner does not agree with the wavelength response quoted for the bleaching of TL signal but is dependent on the chosen illumination time [35]. In this study, the method followed is that discussed by Alexander et al. [19 &20]. By considering the photo-ionization cross section σ_d (eq. 56 chapter 2), the true PTTL wavelength dependence can be obtained. In their numerical simulations it was found that taking the initial slope of the PTTL against illumination time curves $S(\lambda)$ and plotting this against wavelength, the shape of the photo-ionization cross section curve (i.e. true wavelength dependence of PTTL) could be obtained.

Figure 4.17 (a) and (b) shows the PTTL signal as a function of wavelength (λ) with an illumination time selected from the initial linear slope of figure 4.9 (b). The initial time selected was used at all illumination wavelengths. Illumination was maintained at a constant photon flux of $2.59 \times 10^{11} s^{-1} cm^{-2}$ for 1min. Though not included in these results, almost the same behavior as that of figure 4.17 was obtained using 10 minutes illumination time. This supported the content that taking the initial slope provides a good

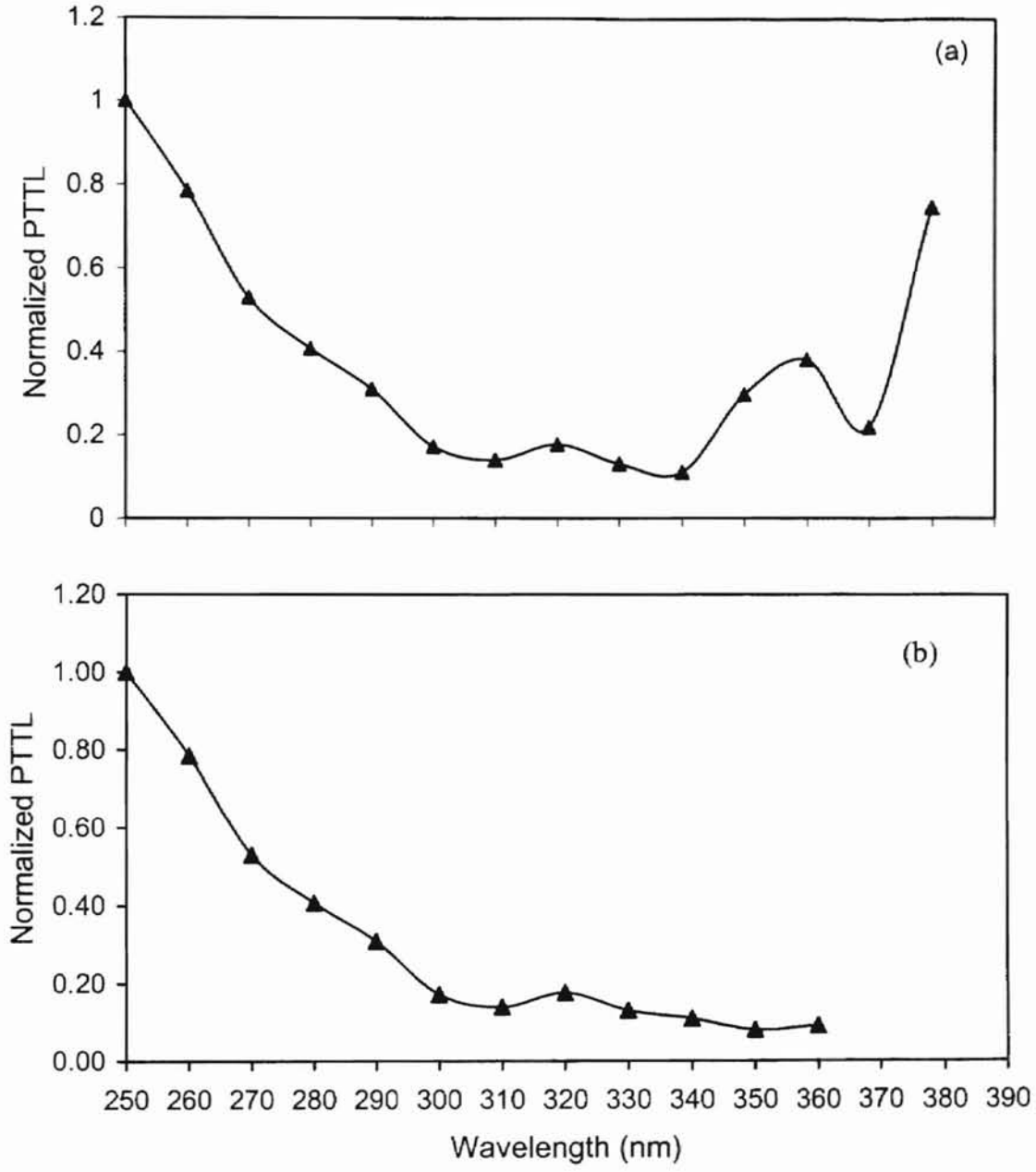

Figure 4.17: PTTL signal as a function of stimulation wavelength for α-Al_2O_3. The sample was illuminated for 1min at a given wavelength. A constant photon flux of 2.5988 x $10^{11}s^{-1}$ cm^{-2} maintained through the illumination. (a) signal with out slide at 350nm and (b) signal with slide starting from 350nm.

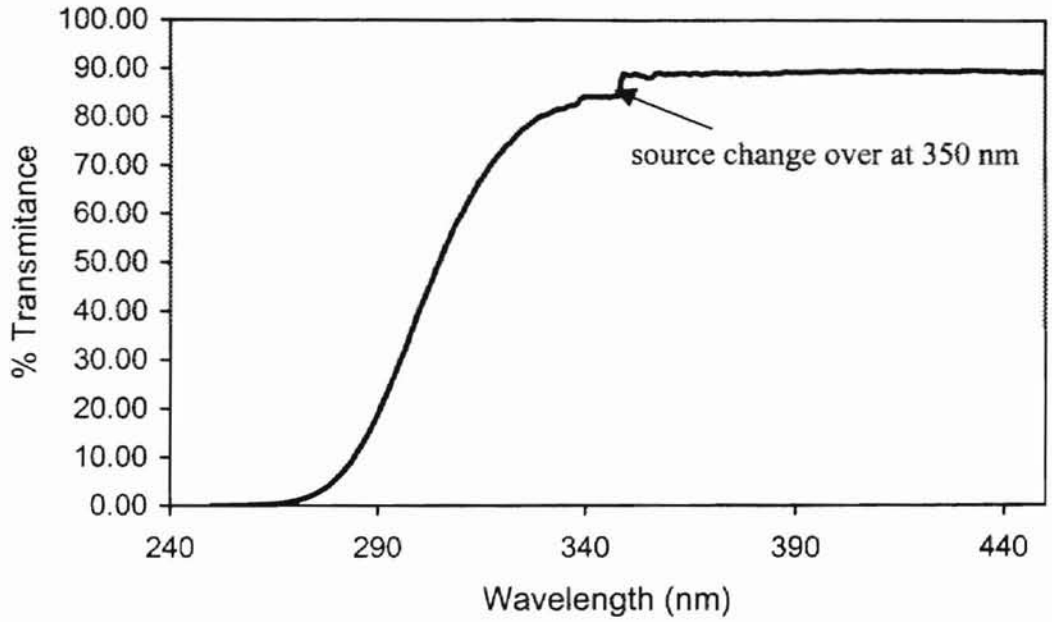

Figure 4.18: Spectral transmitance of the micro slides glass (size 3x1, thickness 0.93 to 1.05mm). Measurement was taken using Cary 500 Spectrophotometer.

estimate of the illumination time. Similar behaviour between the 1min and 10min curve show that the same traps generated the PTTL signal. The data obtained also shows that long wavelengths are not as effective at inducing the PTTL signal as short wavelengths. During the measurement of the PTTL signal versus wavelength dependence, we see second order effects starting at λ<360nm, figure 4.17 (a). This was assumed to be due to absorption by F centers at 205nm. That is illumination with 205nm light releases electrons converting the F centers to the F^+centers ($F \rightarrow F^+ + e^-$ (oxidation)). The released electron becomes trapped in the dosimetry trap yielding TL signal, instead of PTTL. Due to this effect we need to filter out short wavelength light. In an attempt to resolve the latter, a micro seal slide (figure 4.18) was used.

Figure 4.18 provides the spectral transmission curve for a micro slide (size 3 x1 inch, thickness 0.93 to 1.05mm made in U.S.A. of Swiss Glass) used. The glass was mounted at the exit slit of the monochromator. The spectrum was obtained using Cary 500 spectrophotometer. It shows the % transmitance as function of wavelength in the region 250-450nm. The spectrum show that all wavelength <270nm are absorbed by the slide. The feature at 350nm results as the change of source (i.e. from tungsten lamp (visible light) to Deuterium lamp (UV light)) obtained for the glass seal. Figure 4.17 (b) shows the PTTL signal as function of wavelength with micro slide starting at 350nm. The PTTL signal showed a significant decrease in the 350nm. Indeed, it was concluded that the increase in PTTL signal was due to second-order effects.

Figure 4.19 show the comparison of PTTL and photoconductivity as a function and wavelength. During photoconductivity measurements the sample was given an irradiation

of 300Gy ^{60}Co at room temperature and pre-annealed at 473K. The PTTL used is same as in figure 4.19 (b).

Figure 4.20 shows PTTL signal as function of wavelength (integration region 230-330°C) for CaF_2:Cu. The sample was illuminated for 10min at a given wavelength. Illumination time was obtained by taking the initial slope of figure 4.10. A constant photon flux of 2.59×10^{11} s^{-1} cm^{-2} was maintained throughout the illumination. The graph shows that the short wavelengths are effective in inducing PTTL signal in this material. No signal was observed at 300nm. A signal was expected to be seen at this wavelength since the earlier PTTL against illumination results showed some signal. This brings to effect the question of the UV photon flux (light intensity) ϕ used. An increase in the flux causes an increase in the PTTL signal. This can be understood from the equations governing PTTL along with equation (56) from which it is clear that an increase in the illumination intensity causes an increase in the stimulation intensity $f_d=\sigma(\lambda)\phi(\lambda)$. The decrease in the wavelength has similar effect on the PTTL signal. The flux used in this particular case was not enough to induce a signal at this wavelength.

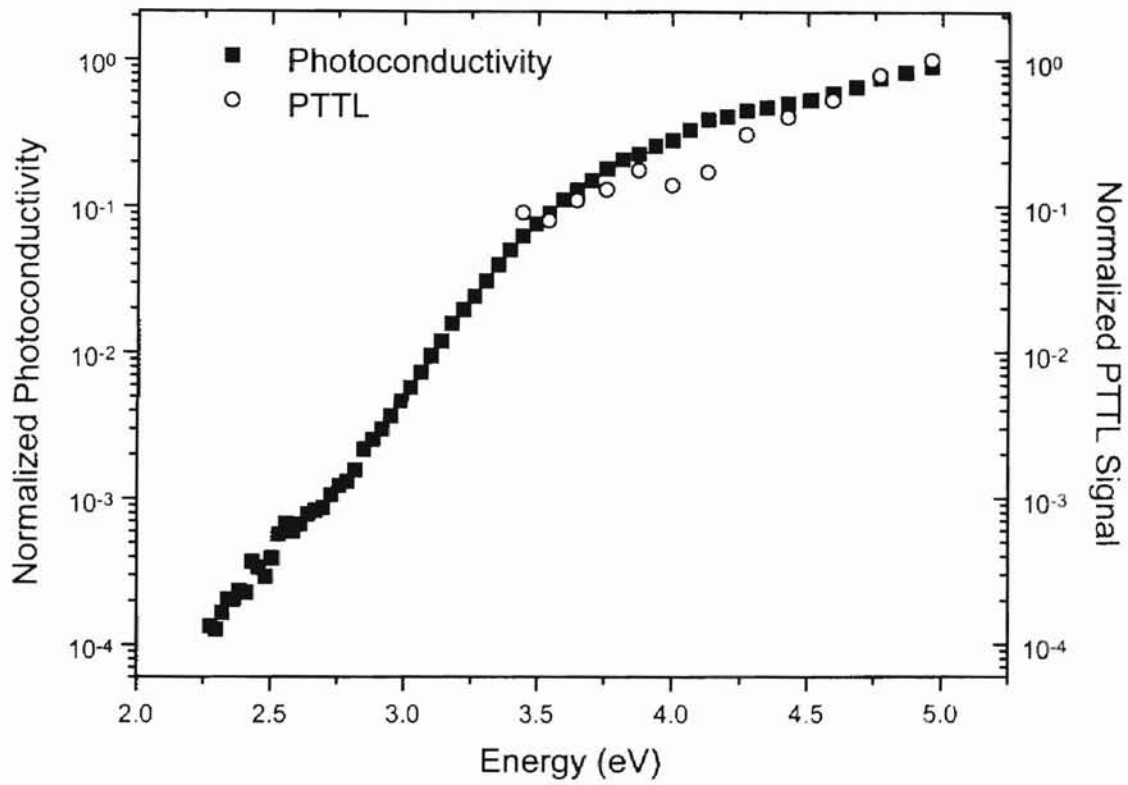

Figure 4.19. Normalized PTTL and Photoconductivity as function of Energy for α-Al_2O_3:C. For photoconductivity sample was irradiated at 300Gy ^{60}Co. Pre-anneal at 473K. For PTTL same irradiation dose 40Gy^{60}Co.

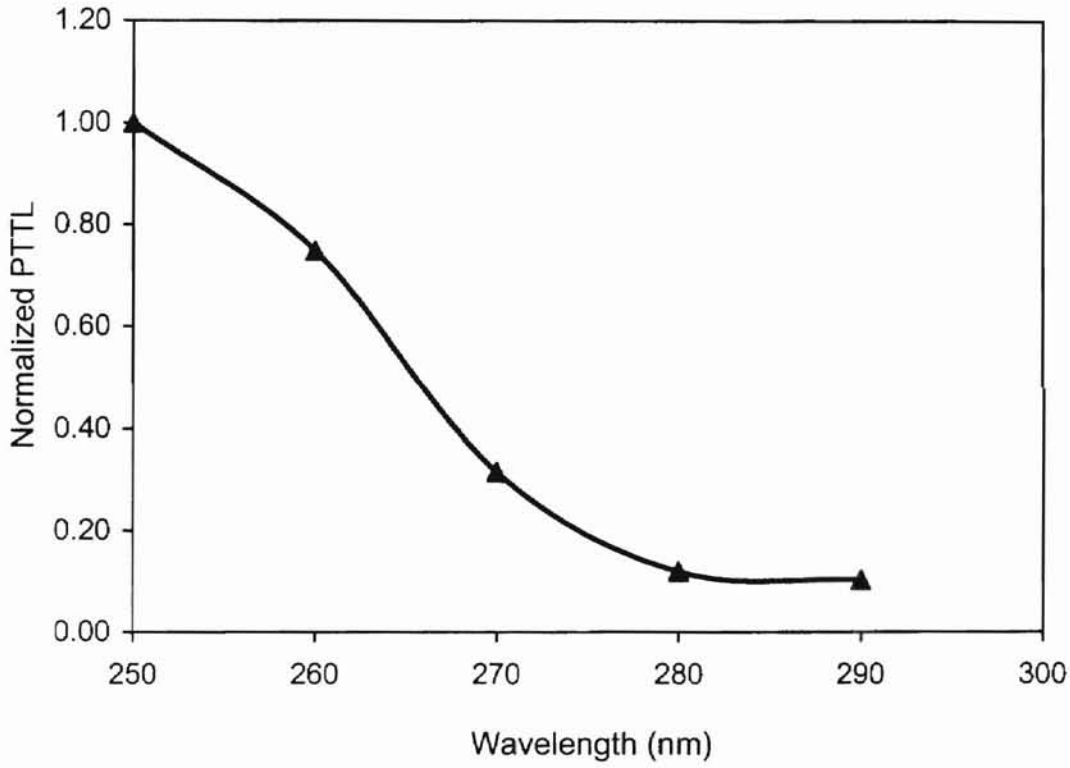

Figure 4.20. PTTL signal as function of wavelength (integration region 230-330°C) for CaF_2:Cu. The sample was illuminated for 10min at a given wavelength. A constant photon flux of 2.59 x 10^{11} s^{-1} cm^{-2} was maintained throughout the illumination.

4.2 Discussion

The TL from α-Al_2O_3 is known to suffer from thermal quenching [20] such that the luminescence efficiency decreases as the temperature increases. This causes the high temperature side of the TL glow curve to be distorted. In principle, correction is necessary before analysis of the TL glow peaks. The correction can be performed using the standard Mott-Seit model of thermal quenching. In this work, however any errors associated with the PTTL measurement caused by thermal quenching are believed to be minor and as a result no attempt was made to account for thermal quenching. Walker et al. [26] noted that TL peaks shift to lower temperatures at higher doses (> ~10Gy), therefore TL peak is less likely affected by thermal quenching in this high dose range (40Gy). The glow peak curve has a low temperature peak at ~50°C sometimes observed just upon irradiation but decays at room temperatures some minutes after irradiation. Recent studies by Agernap Larsen et al. [18] show that the TL curve shapes are the result of a distribution in energy of populated traps. Due to this effect and thermal quenching no fitting of the data was attempted.

The PTTL peaks in α-Al_2O_3 were observed at almost the same position as the TL peak (~190°C) but with reduced intensity. PTTL efficiency is dependent upon annealing temperatures and is much reduced after annealing at temperatures 800-950°C [20,25]. PTTL is due to the transfer of charge from deep donor traps to shallow traps. Colyott [15] argued that the PTTL signal is due to transfer of charge carriers from the deeper traps that become unstable near 630°C and 930°C. In the recent study of F and F^+ centers, Polf [42] showed that the ~180°C TL peak was due to the release of trapped electrons recombining with F^+ center to produce F center. At higher temperatures near ~630°C the reverse

happens. That is the F^+ center increases implying thermal release of hole from these deep traps. A further increase in temperature caused yet another increase in the F^+ center associated with the release of trapped electrons from deep trap. In agreement with their results traps at the ~190°C are electron traps. These results are further backed by Akselrod [20] who assumed a deep hole trap annealed at 550°C and deep electron trap emptied at 900°C. Therefore these deeper traps are assumed as source traps in the PTTL process. That is, PTTL is envoked by optical transfer of electron from the deep traps into the dosimetric traps. Figure 4.9 shows that UV illumination generates as well as bleaches the PTTL glow peaks. This is demonstrated by fact that after attaining a maximum the peak starts to decrease towards zero.

On examining figure 4.14, it's apparent that there are multiple source traps responsible for the PTTL signal in the wavelength region 250-390nm. The spectrum remains almost similar at higher wavelength, whereas at small wavelength (i.e. at high stimulation energies, between 4.0 and 4.9 eV) the PTTL increases more rapidly. The method used to obtain the wavelength dependence agrees with the results by Whitley [41] for photoconductivity (see figure 4.19). By maintaining the stimulation photon flux constant under conditions of weak stimulation, [41] he showed that photoconductivity against wavelength spectra yield directly the dependence of the photo-ionization cross-section as a function of wavelength. The stimulation spectra for OSL and photoconductivity cannot be explained using discrete values for the trapping of energies in the states. The data obtained for photoconductivity were compared with the data for PTTL wavelength dependence. Although the PTTL data were few, the shape of the PTTL wavelength

dependence corresponds well with that of photoconductivity spectra in the range ~3.5eV to ~3.9eV and ~4.3eV to ~4.9eV.

CaF_2:Cu

The history of this material was not known at the time the experiments were performed. As noted in the result, there is no literature about the TL glow peak of CaF_2:Cu shown in figure 4.2. As compared to the TL glow curve (semi-plot) with complex peaks, the PTTL signal coincides with the TL glow curve exposed to the γ source. However the PTTL did not contain all glow peaks except the 303°C present in the induced TL and a hump covered with background at higher temperatures. PTTL transfer is assumed to be due to transfer of charge from deep traps. The deep traps might be hole or electron traps.

The PTTL versus time behavior depicted by figure 4.6 exhibits a monotonic increase with illumination time. The peak seems to be approaching saturation slowly. Similar behaviour was observed by Sunta [34], after studying the PTTL trapped charges related to TL glow peaks at high temperatures (≥500°C) in natural CaF_2. PTTL was observed to increase linearly with time with no appreciable depletion in TL intensity for the low UV flux. In contrast, for high UV flux the PTTL peak followed an increase then started decreasing after attaining a maximum intensity. The decay line (figure 4.14) suggests an intermediate case with some weak depletion of the donor traps.

MgO and MgO:Cu samples

The problem encountered in studying MgO samples is reproducibility of the TL response. The non-reproducibility effect is due to the difference in the equilibrium concentration of the transition metal impurities found in the material [27]. This difference

can be minimized with suitable heat treatment at high temperatures. During irradiation, reaction of the form $Fe^{2+} \rightarrow Fe^{3+} + e^-$ are believed to be taking place [43]. The reverse is true during annealing (i.e. Fe^{3+}/Fe^{2+}).

The TL glow curves obtained for MgO and MgO:Cu exhibits low temperature peaks at ~120°C and 130°C respectively. These peaks are highly sensitive to 40Gy ^{60}Co irradiation than the high temperature peaks. However, they are unsuitable for dosimetry because of their thermal instability. The peaks in the two samples appear to be relatively the same intensity, but peaks in the MgO sample occurs at a later temperature except for the 120°C peak. The MgO peaks are broader than MgO:Cu peaks. The TL glow curves show a variation in the intensity of the peaks. This is in part a reflection of the variation in the impurity content of the sample (i.e. the lower the impurity content the higher the TL intensity). The decrease in the TL intensity with higher impurity is a result of "concentration quenching" [8]. An attempt was made to fit the TL glow curve using first-order model. For MgO:Cu sample, the respective trap energies were ~1.01eV, ~1.0eV and 0.72eV for the ~130°C, ~181°C and ~273°C. The PTTL curves and TL curves were observed at the same temperatures. This suggests that the traps responsible for their production were the same. What is interesting to note is that both samples showed a monotonic increase then reached some saturation level after long illumination.

4.3 Conclusion

It was found that UV light could be utilized for the phototransfer of charges from the deeper traps to the main dosimetry peaks in the used materials. For α-Al_2O_3:C, the deep traps which maybe considered as source traps for PTTL signal induced by UV light were

located near 630°C. F^+ center increases to thermally release holes from the deep traps. Recombination occurs at the electron trap, i.e.180°C trap during PTTL. There is simultaneous optical emptying of charge out of dosimetry trap during UVB illumination. The long wavelength measurements are not as effective at inducing PTTL signal as short wavelength in the region ~250nm-400nm. The response of α-Al_2O_3:C covers a wide range of UV wavelength, while CaF_2:Cu response covers only a range of UVC. The Ultraviolet wavelength of concern for erythema and conjunctivitis are in the range of 250nm to 320nm, therefore α-Al_2O_3:C detectors can be used as UV dosimeter in this region. The traps responsible for the PTTL in CaF_2:Cu and MgO samples were not studied in detail. Further research needs consideration for studying the deep traps responsible for PTTL in these materials. Due to time constraints in preparation of this thesis, the wavelength dependence experiments for MgO and MgO:Cu were not reported. In summary, the dosimeters described in this work possess many attractive features for Ultraviolet Radiation Dosimetry.

References

1. World Health Organization (WHO). *Health and Environmental Effects of Ultraviolet Radiation.* Environmental Health Criteria 160 (3-21) Geneva (1995)
2. Driscoll, C.M.H. *Solar UVR Measurements.* Radiat. Prot Dosim, **64** (3) 179-188 (1996)
3. National Radiological Protection Board (NRPB), *Ultraviolet Radiation* (1993)
4. Mackie, R.M., *Ultraviolet Radiation and the Skin.* Reprint from Radiological Protection Bulletin No 143 (5-9) (1993)
5. McKinlay, A., *UVR Exposure and Human Health*, Reprint from Radiological Protection Bulletin 183 (42-46) (1996)
6. McKeever, S. W. S., Moscovitch, M., Townsend, P.D., *Thermoluminescence Dosimetry Materials: Properties and Uses.* Nuclear Technolgy Publishing (kent). ISBN 1 870965 19 1 (1995)
7. McKeever, S.W.S, *Thermoluminsence*, Encyclopedia of Applied Physics, **21**,355-371, Wiley- VCH Verlag GmbH (1997)
8. McKeever, S.W.S, *Thermoluminsence of Solids.* Cambridge University Press (Cambridge). ISBN 0 521 24520 6. (1985)
9. Randall, J.T. and Wilkins, M.H.F. *Phosphorescence and Electron Traps I. The study of Trap Distributions*. Proc. Roy. Soc. (London) **A184**(A999), 366-389(1945)
10. Randall, J.T. and Wilkins, M.H.F. *Phosphorescence and Electron Traps II. The Interpretation of Long-Period Phosphorescence*. Proc. Roy. Soc. (London) **A184**(A999), 390-407(1945)
11. Chen, R. and McKeever, S.W.S., *Theory of Thermoluminescence and Related Phenomena*. World Scientific Publishing Co. Pte. Ltd. ISBN 9810222955. (1997)
12. McKeever, S.W.S, and Chen, R, *Luminescence models*, Radiat. Meas.**27**, (5/6), 625-661. (1997)
13. Garlick, G.F.J. and Gibson, A.F. *The Electron Trap Mechanism of Luminescence in Sulphide and Silicate Phosphors*. Proc. Phys. Soc. (London) **A60**(6), 574-590 (1948)
14. May, C.E. and Patridge, J.A., *Thermoluminescent Kinetics of Alpha Irradiated Alkali Halides*. J. Chem. Phys. **40**, 1401-1409 (1964)
15. Colyott, L.E, Akselrod, M.S and McKeever S.W.S, *Phototransfer Thermoluminescence in α-Al_2O_3:C,* Radiat. Prot. Dosim. **65** (1-4), 263-266 (1996), Nuclear Technology Publishing
16. Colyott, L.E., Akselrod, M.S and McKeever S.W.S, *An integrating Ultraviolet-B Dosimeter using Phototransfered Thermoluminescence from α-Al_2O_3:C,* Radiat. Prot. Dosim. **72**(2)87-94(1997)
17. Bulur, E., and Göksu, H.Y., *Phototransfered Thermoluminescence from α-Al_2O_3:C using blue light emitting diodes.* Radiat. Meas. **30**, 203-206.(1990)

18. Agersnap Larsen, N., Bϕtter-Jessen, L., and McKeever, S.W.S, *Thermally Stimulated conductivity and thermoluminescence from Al_2O_3:C*, Radiation Protection Dosimetry **84**, Nos 1-4, 87-90(1999)

19. Alexander, C.S., and McKeever, S.W.S., *Phototransfer Thermoluminescence*, J Phys. D; Appl. Phys. **31** 2908-2920 (1998)

20. Akselrod, M.S., and Gorelova, E.A. *Deep Traps in highly sensitive α-Al_2O_3:C TLD crystal.* Nucl. Track Radiat. Meas. **21**(1) 143-146. (1993)

21. Oster, L., Weiss, D., and Kristianpoler, N., A Study of Photostimulated Thermoluminescence in C-doped *α-Al_2O_3:C.* J. Phys. D. Appl. Phys **27**, 1732-1736.

22. Wintle, A.G. and Murray, A.S., Radiat. Meas. **27**, 611

23. Akselrod, M.S., Kortov, V.S., Kravetsky, D.J. and Gotlib, V.I., *Highly sensitive Thermoluminescence Anion_Defective α-Al_2O_3:C single crystal Detectors.* Radiat. Prot. Dosim. **32**(1)15-20(1990)

24. Akselrod, M.S., Kortov, V.S., Kravetsky, D.J. and Gotlib, V.I., *Highly sensitive Thermoluminescence Anion_Defective α-Al_2O_3:C single crystal Detectors.* Radiat. Prot. Dosim. **33**(1)119-122(1990)

25. Colyott, L.E., *Dosimetric Properties of α-Al_2O_3:C exposed to ionizing and non-ionizing Radiation.* PhD. Dissertation, Oklahoma State University (1997)

26. Walker, F.D., Colyott, L.E, Agersnap Larsen, N. and McKeever, S.W.S., *The Wavelength Dependence of light Fading of Thermoluminescence from α-Al_2O_3:C*, Radiat. Meas. **26**(5)711-718 (1996)

27. Las, W.L., Matthews, R.J., and Stoebe, T.G., *Mechanisms for Thermoluminescence in MgO and $CaSO_4$* Nucl. Instr and Methods **175,**1-3 (1980)

28. Las, W.C. and Stoebe, T.G., *Effect of the Equilibrium Concentration of Impurities on the Reproducibility of Thermoluminescence in MgO* J. Materials Science **16** 1191-1196 (1981)

29. Okuno, E and Watanabe, S. *U.V. Induced Thermoluminescence on Natural Calcium Fluoride. Health Phys.* **23**(9) 377-382(1972)

30. Agersnap Larsen, N, Dosimetry Based on *Thermally Stimulated Luminescence.* PhD Dissertation University Of Copenhagen. (1997)

31. Takeuchi, N., Inabe, K., Yamashita, J., and Nakamura, S., *Thermoluminesnce of MgO Single Crystals for U.V. Dosimetry*. Health Phys. **31** 519-521 (1976)

32. Las, W. C. and Stoebe, T.G., *Thermoluminescent Mechanisms involving the transtions Metal Ion Impurities and V-type centres in MgO Crystals exposed to Ultraviolt Radiation*, J. Materials Science **17** 2585-2593 (1982)

33. Justus, B.L., and Huston A.L., *Ultraviolet Dosimetry Using Thermoluminescence of Semiconductor-doped Vycor Glass*. Appl. Phys. Lett. **67** (9) 28 (1995)

34. Sunta, C.M., Mechanism of *Phototransfer of Thermoluminescence Peaks in CaF_2.* Phys. Stat. Sol. (a) **53** 127-135 (1979)

35. Alexander, C.S., Morris, M.F., and McKeever, S.W.S., *The Time and Wavelength Response of Phototransfer Thermoluminescence in Natural and Synthetic Quartz.* Radiat. Meas. **27** (3) 153-159 (1997)

36. Pradhan, A.S., and Bhatt, R.C. *Dose Dependence of Photo-transfer Thermoluminescence in $CaSO_4$:Dy.* J.Phys. D: Appl. Phys., **18** 317-320 (1985)

37. Kharita, M.H., Stokes, R., and Durrani, S.A., *Phototransfer Thermoluminescence (PTTL) in LiF (Mg, Cu, P) (GR-200)*, Radiat. Meas. **23**, Nos2/1 493-496 (1994)

38. Bøtter-Jensen, L. and Mejdahl, V. *Microcomputer-controlled Reader System for Archaelogical and Geological TL Dating*: Nucl. Radiat. Protect. Dosim. **6**, 193-196 (1984)

39. Bøtter-Jensen, L. *The Automated Riso TL Dating Reader System*: Nucl. Tracks Radiat. Meas. **14**, 177-180 (1988)

40. Bøtter-Jensen, L. and Duller, G.A.T. *A New System for Measuring OSL from quartz Samples*. Radiat. Meas. **20** 549-553 (1992)

41. Whitley, V.H., McKeever, S.W.S., *Photoionization of Deep Center in Al_2O_3*, J. Appl. Phys. **87**(1)249-256 (2000)

42. Polf, J.C., *The Role of Oxygen Vacancies in Thermoluminescence Process in Al_2O_3.* MS. Thesis, 2000

43. Kortov, V.S., Milman, I.I, Monakhov, A.V., Slesarev, A.I., *Combined TSL-ESR MgO Detectors for Ionising and UV Radiations.*, Radiat. Prot. Dosim. (1993)

VITA

Dick Andries Sono

Candidate for the Degree of

Master of Science

Thesis: POTENTIAL TLD MATERIALS FOR USE AS ULTRAVIOLET RADIATION DOSIMETERS

Major Field: Physics

Biographical:

Personal Data: Born in Hammanskraal, South Africa on April 05, 1970, the son of Thomas M. and Lati V. Sono

Education: Graduated from Hans Kekana High School, Temba, South Africa in December 1988; received Bachelor of Science in Education and Bachelor Science Honours degree in Physics from University of North West Mafikeng, South Africa in December 1995 and 1996 respectively. Completed the requirements for the Master of Science degree in Physics at Oklahoma State University in May, 2000.

Experience: Employed by University of North West, as an undergraduate lab assistant and graduate lab assistant 1995 and 1996 respectively. Employed as a junior lecturer by University of North West, 1997 to present.

Professional Membership: South African Institute of Physics.